Unraveling the Pleomorphic Forms of *Borrelia burgdorferi*

Anni Herranen

Master's thesis

University of Jyväskylä

Department of Biological and Environmental Sciences

Cell and Molecular Biology

09.10.2014

Preface

For this journey to the fascinating world of *Borrelia*, I own thanks to my instructor Dr. Leona Gilbert. Special thanks go also to MSc Leena Meriläinen for all the help in laboratory work and writing. Furthermore, I want to thank the whole LEE's group for support and for sharing a good time (and plenty of cake) at the office.

Jyväskylän yliopisto
Matemaattis-luonnontieteellinen tiedekunta

Pro gradu –tutkielman tiivistelmä

Tekijä: Anni Herranen
Tutkielman nimi: *Borrelia burgdorferin* eri esiintymismuotojen tarkastelua
English title: Unraveling the pleomorphic forms of *Borrelia burgdorferi*
Päivämäärä: 09.10.2014 **Sivumäärä:** 49

Laitos: Bio- ja ympäristötieteiden laitos
Oppiaine: Solu- ja molekyylibiologia
Tutkielman ohjaaja(t): Leona Gilbert, Leena Meriläinen

Tiivistelmä:

Borrelia burgdorferi bakteeri on puutiaisten välittämän borrelioosin taudinaiheuttaja. Tämä tavanomaisesti spirokeettana esiintyvä bakteeri kykenee vaihtamaan muotoaan ympäristöolosuhteiden muuttuessa epäsuotuisiksi. *Borrelia*-bakteerin eri esiintymismuotojen uskotaan olevan borrelioosin pitkittyneen taudinkuvan takana, minkä vuoksi näiden muotojen tutkiminen on tärkeää. Tämän pro gradu –työn tavoitteena oli tutkia *B. burgdorferin* pleomorfisia muotoja ja löytää muotoja erottavia morfologisia tekijöitä sekä eroja proteiiniekspressiossa ja borrelioosipotilasseerumivasteessa spirokeettojen ja pyöreän esiintymismuodon välillä. Olettamuksena oli, että konfokaalimikroskopialla muotojen väliltä löydetään rakenteellisia eroja lipidi- ja hiilihydraattiarkkitehtuurissa. Myös proteiiniekspression ja borrelioosipotilaiden seerumivasteen oletettiin olevan yksilöllinen kullekin muodolle. Kollageeniin sitoutuva Acid Fuchsin –väri värjäsi ainoastaan biofilmejä, kun taas N-asetyyliglukosamiineihin sitoutuva WGA-väri (Wheat Germ Agglutinin) tarttui vain vedellä aikaansaadun pyöreän esiintymismuodon (round body) pinnalle. WGA-värjäyksen tulos viittaa peptidoglykaanin paljastumiseen bakteerin ulkopinnalla pyöreässä esiintymismuodossa. Läpäisyelektronimikroskooppikuvista koottiin kuvasarja mallintamaan spirokeetan laskostumista pyöreään esiintymismuotoon. Lisäksi näistä kuvista tarkasteltiin kaksoiskalvorakenteen ja flagellojen säilymistä pyöreässä esiintymismuodossa ja havaittiin neljän päivän inkuboinnin ihmisen seerumissa aiheuttavan muodon muutoksen pyöreään esiintymismuotoon. Lisäksi ihmisen seerumin havaittiin aiheuttavan runsasta vesikkelien eritystä sekä protoplasmisen sylinterin turpoamista. Flagellan säilyminen pyöreässä esiintymismuodossa todettiin lisäksi immunoleimaamalla flagella p41 -vasta-aineella. Flagellan säilyminen ja vesikkeleiden eritys viittaavat siihen, että pyöreä esiintymismuoto kykenee aiheuttamaan immuunivasteen. Lisäksi WGA-värjäys todisti ainakin toisen soluseinän pääkomponentin, N-asetyyliglukosamiinien, esiintymisen myös pyöreässä esiintymismuodossa. Näin ollen tulokset haastavat olettamuksen, että pyöreä esiintymismuoto olisi soluseinätön. Spirokeettojen ja pyöreän esiintymismuodon proteiiniprofiileja verrattiin keskenään kaksiulotteisella geelielektroforeesilla, eikä pyöreän esiintymismuodon proteiinimäärän havaittu olevan pienempi kuin spirokeettojen, mitä olisi voitu olettaa mikäli ulkokalvo olisi vahingoittunut. Sen sijaan havaittiin useiden 15-40 kDa proteiinien ekspression olevan suurempi pyöreässä esiintymismuodossa. Spirokeettojen ja pyöreiden esiintymismuotojen antigeenisyyttä vertailtiin borrelioosipotilasseerumien avulla. Vasta-aineet näyttivät vaihtelevan voimakkaasti seerumien välillä. Kuitenkin muodot aiheuttivat selkeästi erotettavat, yksilölliset immuunivasteet, mikä viittaa myös pyöreän esiintymismuodon olevan kliinisesti merkittävä muoto. Useat kokeessa käytetyistä seerumeista näyttivät reagoivan voimakkaammin pyöreän esiintymismuodon proteiinien kanssa. Näiden kokeiden pohjalta on mahdollista jatkaa työvälineiden valmistelua *B. burgdorferin* eri esiintymismuotojen yksilölliseksi tunnistamiseksi, mikä voisi parantaa bakteerin havainnointia borrelioositesteissä.

Avainsanat: *Borrelia burgdorferi*, borrelioosi, flagella, ihmisen seerumi, pleomorfia

University of Jyväskylä
Faculty of Mathematics and Science

Abstract of Master´s Thesis

Author: Anni Herranen
Title of thesis: Unraveling the pleomorphic forms of *Borrelia burgdorferi*
Finnish title: *Borrelia burgdorferin* eri esiintymismuotojen tarkastelua
Date: 09.10.2014 **Pages:** 49

Department: Department of Biological and Environmental Sciences
Chair: Cell and Molecular Biology
Supervisor(s): Leona Gilbert, Leena Meriläinen

Abstract:

Lyme disease is caused by *Borrelia burgdorferi* bacteria and typically diagnosed by an erythema migrans rash. As the disease develops it becomes more challenging to diagnose. Pleomorphic forms might be responsible for the prolonged disease profile, even though much controversy exists about them. Thereby the aim of this study was to examine the pleomorphism of *B. burgdorferi*. The hypothesis is that each pleomorphic form has specific morphological traits and unique antigenicity. Protein expression is also different in spirochetes and round bodies (RBs). The collagen dye Acid Fuchsin stained only biofilms whereas N-acetyl glucosamine dye wheat-germ agglutinin (WGA) stained RBs. WGA staining illustrated that one of the main components of bacterial cell wall, N-acetyl glucosamines, are still present in RBs and indicated that peptidoglycan would become exposed at the surface of RBs. Human serum induced RB formation suggesting that this form has physiological significance. Transmission electron microscope (TEM) images lead to a model demonstrating how the spirochetes could fold into RBs. The presence of flagella in the RBs was examined by immunolabeling with flagellar antibody p41. TEM images of human serum induced RBs revealed increased vesicle formation and swelling of protoplasmic cylinders. Undamaged phospholipid bilayers were observed in RB TEM images. In addition, protein profiles of spirochetes and H_2O RBs were analyzed with two-dimensional polyacrylamide gel electrophoresis (2D PAGE). Analysis of the protein profiles did not reveal a decrease in the overall protein expression of RBs, which might have been expected if this form would have a damaged outer cell wall. Instead, an increase of the expression of several proteins of molecular weight 15-40 kDa was observed in the RBs. These proteins might be needed for adjusting to the unfavorable environmental conditions. Antigenicity of spirochetes and RBs were compared by western blots immunolabeled with Lyme patient sera. The blots demonstrated that RBs could induce an immune response. Moreover, the immune response is different from spirochetes. However, the antigen-antibody response seemed to vary greatly depending on the serum. Still, RBs could be clinically important since their antigenicity differs from the parent spirochete form. These findings could provide tools for the specific detection of pleomorphic forms of *B. burgdorferi* benefiting the diagnosis of Lyme disease.

Keywords: *Borrelia burgdorferi*, flagella, human serum, Lyme disease, pleomorphism

Table of contents

Abbreviations

2D PAGE	Two-dimensional polyacrylamide gel electrophoresis
Bb	*Borrelia burgdorferi*
Bodipy	boron-dipyrromethene
BSA	Bovine serum albumin
BSK-II	Barbour-Stoenner-Kelly culture medium
CDC	Centers for Disease Control and Prevention
DAPI	4', 6-diamidino-2-phenylindole
DIC	Differential interference contrast
DMA	N, N-dimethylacrylamide
DTT	DL-dithiothreitol
ELISA	enzyme-linked immunosorbent assay
EtBr	Ethidium bromide
GluNAc	N-acetyl glucosamine
IPG	immobilized pH gradient
MES	2-[N-morpholino]ethanesulfonic acid
Osp	Outer surface protein
PCR	Polymerase chain reaction
PI	Propidium iodide
PTA	Phosphotungsted acid
RB	Round body
RCF	Relative centrifugal force
RT	Room temperature
SDS	Sodium dodecyl sulphate
TBS	Tris-buffered saline
TEM	Transmission electron microscope
WGA	Wheat germ agglutinin

1 Introduction

Tick-borne Lyme disease is currently the most common vector-borne illness in the western world (Schnarr *et al*., 2006). The number of reported cases has almost doubled both in the USA and Finland in 12 years (see Table 1). The causative agent of the disease is the bacterium *Borrelia burgdorferi* (Bb) (Burgdorferi *et al*., 1982). Although Lyme disease is rarely life-threatening, it causes significant problems for the infected individuals, especially if left untreated (Schnarr *et al*., 2006).

Table 1: Increasing prevalence of Lyme disease. The rising number of reported Lyme disease cases in the USA and Finland, years 2000 and 2012.

Reported Lyme disease cases	2000	2012
USA*	17,700	30,800
Finland**	900	1,600

* CDC, Centers for Disease Control and Prevention, USA
** National Institute for Health and Welfare, Finland

The development of Lyme disease can be divided into early, disseminated, and late stages (Schnarr *et al*., 2006). A detectable characteristic of Lyme disease in the early localized stage is a specific rash, erythema migrans, which develops around the tick bite. Other symptoms caused by the Lyme disease in the early stage can be diverse, including for example low-grade fever like symptoms, dysphasia, headaches, impaired vision and hearing, and fatigue (for review see Girschick *et al*., 2009). In the dissemination stage, common symptoms may include acute neuroborreliosis, secondary annular skin lesions, migratory musculoskeletal pain or heart and eye problems (Schnarr *et al*., 2006). Persisting or recurring arthritis and encephalomyelitis are signs of the late manifestations of Lyme disease (Feder *et al*., 2006). Usually, Lyme disease can be cured with antibiotics. However, in some cases symptoms stay even after proper antibiotic treatment (Kersten *et al*., 1995; Feder *et al*., 2006; Schnarr *et al*., 2006). These "post-Lyme" or chronic symptoms range from fatigue, arthralgias, muscoskeletal or radicular pain, paresthesia, and neurocognitive impairment to mood disturbances (Schnarr *et al*., 2006). Additionally, Schnarr *et al*. (2006) suggested the term "treatment-resistant Lyme disease" if typical Lyme disease symptoms, such as arthritis, persist longer than one year.

Diagnosis of Lyme disease is repeatedly based on the rash, erythema migrans, even though the rash might be absent or stay easily unnoticed in some patients (Nau *et al*., 2009; Stanek *et al.*, 2012). Early detection without the rash is difficult, since commonly used enzyme-linked immunosorbent assay (ELISA) and western blot tests are based on antibodies, and reaching detectable levels of antibodies takes weeks (Feder *et al*., 2006). Cultivation of Bb from patient samples is also challenging and polymerase chain reaction (PCR) based analysis is not reliable in the long run, since the persistence of Bb DNA does not confirm the viability of the bacteria (Brorson and Brorson, 1997; Iyer *et al*., 2013). Early detection would be beneficial for successful treatment hence better diagnostic tools are needed for accurate and sensitive identification of Lyme disease in all of its phases.

Further information about the unique bacterium responsible for Lyme disease is needed. How can the apparently simple spirochete survive the vast change in the environmental conditions when it gets transferred from the tick mid-gut to a mammalian host? In addition, Bb faces the same problems as any invading pathogen: the host's immune system. To survive, Bb has to have means to cope with the host's defense, such as changing its shape or altering its protein expression. The role of the controversial pleomorphic forms of Bb are still under debate (Miklossy *et al*., 2008; Lantos *et al*., 2014). Additionally to the parental spirochete form, Bb has repeatedly been observed in a spherical shape or forming large colonies containing numerous bacteria, biofilms (Aberer and Duray, 1991; Brorson and Brorson, 1997; Alban *et al*., 2000; Miklossy *et al*., 2008). However, these forms are not accurately described yet and their meaning remains unsolved. Thereby, in this Master's thesis the focus is on the pleomorphism of Bb to specify the morphological traits of the different forms.

1.1 The vector and the pathogen

Ticks from the genus *Ixodes* serve as the vector for *B. burgdorferi*, *I. ricinus* mainly in *Europe* and *I. scapularis* in America (Adelson *et al*., 2004; Michelet *et al*., 2014). The spirochetes reside in the tick mid-gut in a dormant stage (Burgdorferi 1982; Schnarr *et al*., 2006). Three Lyme disease causing species of *Borrelia*: *B. burgdorferi sensu stricto, B. garinii* and *B. afzelii*, are commonly referred as *B. burgdorferi sensu lato* (Girschick *et al*., 2009). All three of these Bb species are found in Europe and Asia, but only *B. burgdorferi*

sensu stricto is discovered in the USA. The disease profiles of Lyme disease patients have repeatedly been associated to certain *Borrelia* species. *B. burgdorferi sensu stricto* causes mainly arthritis, *B. garinii* neurological symptoms whereas *B. afzelii* is mainly responsible for skin disorders (Busch *et al*., 1996; Picken *et al*., 1998; Jaulhac *et al*., 2000).

1.2 The structure of *B. burgdorferi*

Bb bacteria have a flat-wave spirochetal shape (Goldstein *et al*., 1996). The spirochetes' length is approximately 10–30 µm and they are 0.2–0.3 µm in diameter (Burgdorfer *et al*., 1982; Hovind-Hougen, 1984). The spirochetes contain a protoplasmic cylinder and an outer membrane surrounded by a slime layer, leaving a periplasmic space between the two lipid bilayers (Barbour and Hayes, 1986; Kudryashev *et al*., 2009). The protoplasmic cylinder contains the bacterium's nucleic acids. The slime layer surrounding the outer membrane might consist of proteins taken up from the medium (Kudryashev *et al*., 2009). The periplasmic space contains a peptidoglycan layer and two bunches of flagella originating from the ends of the spirochete, responsible for the movement of Bb (Fraser *et al*., 1997; Barbour and Hayes 1986). Unlike in many bacteria, even in many spirochetes, the shape of the Bb is not determined by the peptidoglycan layer (Motaleb *et al*., 2000). Instead, flagella participate in the spirochetal shape formation of Bb, while peptidoglycan is responsible for the rod shape of the protoplasmic cylinder (Goldstein *et al*., 1996; Motaleb *et al*., 2000). The amount of flagella differs between the strains of Bb, for example, strain B31 has typically eleven or seven flagella (Hovind-Hougen, 1984) although the number of flagella can also vary within the species (Kudryashev *et al*., 2009). The flagella are located in between the peptidoglycan layer and the outer membrane (Johnson *et al*., 1984). Bb is usually described as a gram negative bacterium even though it lacks, for example, lipopolysaccharides from its outer membrane (Takayama *et al*., 1987; Aberer and Duray, 1991; Fraser *et al*., 1997).

1.3 Flexible genome and protein expression of *B. burgdorferi*

Bb has a rare linear chromosome as well as several linear and circular plasmids (Ferdows and Barbour, 1989; Fraser *et al*., 1997). All Bb species share similarities in their genomes, but the plasmid amount and identity varies even among the strains (Elias *et al*., 2002). No commonly known virulence-factors have been identified in Bb species (Fraser *et al*.,

1997). On the other hand, several lipoproteins, such as outer surface proteins (Osps), which are potentially able to trigger mammalian innate immune system, have been found, (reviewed by Schröder *et al*., 2008). In addition, the glycolipids of Bb, such as cholesteryl 6-O-acyl-β-D-galactopyranoside, are capable of inducing an adaptive immune response (Schröder *et al*., 2003). The whole genome of Bb is small, probably contributing to the fact that it is an obligate parasite. Bb is void of classically-defined machinery for synthesizing nucleotides, amino acids, fatty acids and enzyme cofactors, all of which it thereby needs to scavenge from the host (Fraser *et al*., 1997). This also explains the need of a complex growth medium used for *in vitro* culturing.

Bb seems to possess a remarkable ability to adjust its protein expression according to its environment. An exceedingly studied example is provided by Osps. A 31 kDa protein, OspA, is prevalent on the surface of the spirochete while it resides in the tick mid-gut whereas its expression has been observed to diminish greatly when the spirochete enters a mammalian host (Montgomery *et al*., 1996). Meanwhile the expression of OspC, a 23 kDa protein, increases as the tick is feeding on mammalian blood (Schwan *et al*., 1995; Montgomery *et al*., 1996). OspA likely helps Bb to attach to the tick mid-gut, whereas the expression of OspC leads the spirochetes to move to the salivatory glands for transmission to the mammalian host (Schwan *et al*., 1995; de Silva *et al*., 1996; Pal *et al*., 2004). On the other hand, Grimm *et al*. (2004) observed that OspC was not obligatory for the migration of Bb inside the tick, although it was shown to be essential for the infection of the mammalian host (mouse).

1.4 Pleomorphism of *B. burgdorferi*

Bb is capable of adopting not only the vegetative spirochete form (Figure 1A), but also a spherical form (Figure 1C) or it can be seen forming floating aggregates of spirochetes: biofilms (Figure 1B). Blebs are another form that Bb seems to possess (Aberer and Duray, 1991). However, since blebs seem more likely to be an intermediate form between spirochete and the spherical shape it is not further discussed here. Blebs were included in the structural comparison of the pleomorphic forms (see Results Figure 2) for a closer examination of this intermediate stage. The bacteria switch into the spherical round body (RB) form when environmental factors become unfavorable, for example in serum-starved

conditions or during incubation in H_2O (Brorson and Brorson, 1998). The formation of biofilms is another common way of bacteria to survive unfavorable environmental conditions (Lembre *et al*., 2012). Biofilms consist of aggregates of bacterial cells within an extracellular matrix of polymeric substances (Lembre *et al*., 2012), and Sapi *et al*. (2012) indicated that Bb aggregates fulfill the characteristics of biofilms. However, much inconsistency exists about the nomenclature, characteristics, and the role of the pleomorphic forms of Bb (for review see Stricker and Johnson, 2011). In many articles, the spherical shaped form of Bb is regarded as a cell wall deficient form or a cyst (Bruck *et al*., 1995; Mursic *et al*., 1996). In addition, other round morphological structures derived from Bb, such as vesicles of varying sizes, have been misleadingly termed in a similar way to this pleomorphic form. Blebs and vesicles, starting from size 50 nm in diameter, are sometimes referred to as spherical structures (Lantos *et al.*, 2014). For example Brorson and Brorson (1997), described spherical structures having a diameter of 0.5–2 µm, and still as late as in 2011 Sapi *et al*. (2011) counted both RBs and granules (vesicles) as RB forms in their experiments.

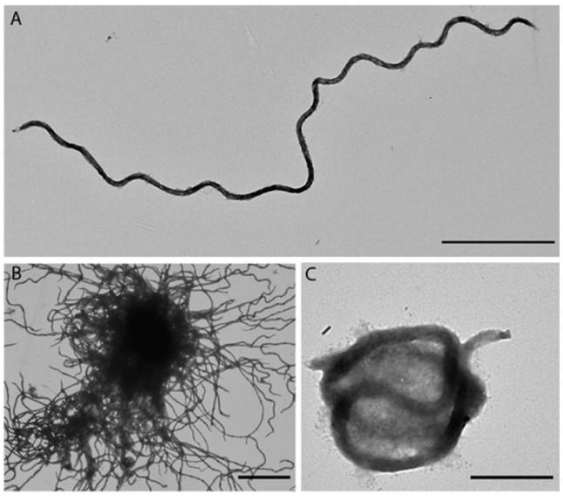

Figure 1: The pleomorphic forms of *B. burgdorferi*. Representative transmission electron microscope images of the pleomorphic forms of Bb B31. Vegetative spirochete form (A), a biofilm (B) and 2h H_2O induced round body (C). All samples were prepared with the negative stain phosphotungsted acid (PTA). Scale bars (A) 5 µm, (B) 10 µm and (C) 1 µm.

The pleomorphic forms of Bb have been suggested a role in chronic Lyme disease (Miklossy *et al*., 2008; Stricker and Johnson, 2011). However, as of now, there is not enough evidence to attest immunological significance of RBs in Lyme disease (Lantos *et al*., 2014). On the other hand, even the definition of RBs has never been thoroughly clarified. In this Masters' thesis, RBs (Figure 1C) refer to a pleomorphic form of Bb with a

diameter of 2.8 ± 0.46 µm (Meriläinen's manuscript, 2014), which possesses a conserved double membrane structure. This view is in accordance with Brorson and Brorson (1997), who examined RB structures of Bb and described them having a double membrane, flagella, and macromolecular substances.

1.5 Detection of *B. burgdorferi*

Especially in the absence of erythema migrans rash itself or its detection, the diagnosis of Lyme disease becomes challenging. Two tier testing with ELISA and western blots (IgM in the early phase or IgG after the first weeks of infections) are used for the diagnosis of Lyme disease (Feder *et al*., 2006). The approximations of the sensitivity and specificity of the two-tier testing vary greatly, from 44%–56% to 83%–95% (Dressler *et al*., 1993; Stricker and Johnson, 2011). However, serological antigenicity tests have some drawbacks since patients with past Lyme disease often stay seropositive for years even after proper treatment with antibiotics (Dressler *et al*., 1993; Schnarr *et al*., 2006). In addition, the production of antibodies takes time, so the tests might not work in the early phase of the disease.

However, as all pathogens, to persist in the mammalian host Bb must have ways to avoid the host's immune defense, which includes adaptation of the protein expression, and thereby raises challenges to the detection of the bacteria and Lyme disease vaccine preparation. For example, the alternating expression of the numerous lipoproteins of Bb misleads the host's immune response: Antibodies are prepared against the Bb antigens, which are presented at the surface of Bb at the beginning of the infection, but Bb changes the expression of its antigens after the invasion (Schwan *et al*., 1995; Schnarr *et al*., 2006). Thereby, the antibodies prepared in the early phase of the attack are not effective anymore. Liang *et al*. (2002) discovered that the anti-OspC antibodies prepared by the adaptive immune system were able to either induce down-regulation of OspC on Bb, or select OspC negative phenotypes of the bacteria, hence decreasing the amount of bacteria towards which the antibodies would be effective. As for the innate immune response, Bb might escape from the complement mediated killing by expressing complement-binding factors (Kraiczy *et al*., 2001). Binding to host molecules might also aid the bacterium to avoid the host's defense. For example, Bb possesses decorin binding proteins, which aid the

bacterium to attach to collagen since decorin is the major component of extra-cellular matrix and binds to collagen (Liang *et al*., 2004). By binding to collagen, Bb could hide from the immune system in the connective tissue.

Pleomorphism might be another way of Bb to hide from the immune defense (Brorson and Brorson, 1997). Commonly used antibodies directed to surface antigens of Bb do not react with RBs, probably because the cell envelope of RBs presents different antigens than the parent spirochete form. Alban *et al*. (2000) observed differences in the protein expression as well as in the antigenicity of Bb spirochetes and RBs. These differences might explain why the diagnosis of Lyme disease can be challenging even in the case of an obvious infection (Brorson and Brorson, 1997).

One basic diagnostic method to detect Bb from patient samples is cultivation. However, it can sometimes take up to three months until growth is observed, and even then, growth is not always detected (Brorson and Brorson, 1997). If RBs have been incubated for weeks, it takes a long time for them to revert back to spirochetal form, which might explain the long incubation time required for the cultivation of Bb from patients. Furthermore, the low metabolic activity of RBs might rescue them from antibiotic treatment (Brorson *et al*., 2009).

2 Aims of the study

Research on the pleomorphism of Bb is needed to clarify the characteristics of the forms and to unify the nomenclature in use. Thereby, the aim of this Master's thesis was to examine the structural similarities and differences between the pleomorphic forms of Bb. Confocal microscopy was carried out to observe the morphological traits of Bb spirochetes, RBs and biofilms. Structural details of Bb were extensively studied with transmission electron microscopy (TEM). Protein profiles and antigenicity of Lyme disease patient sera of spirochetes and H_2O induced RBs were compared to reveal their differences. The hypothesis is that there are structural differences distinguishing spirochetes from RBs and biofilms, and each of them have individual protein patterns as well as antigenicity. In addition, RBs are able to induce an immunological response that is different from the spirochetes.

3 Materials and methods

3.1 Bacterial sample preparation

Infectious *B. burgdorferi* B31 cells from ATCC (ATCC 35210, Manassas, USA) were grown in suspension in Barbour-Stoenner-Kelly (BSK-II) medium (Barbour, 1984) supplemented with 6% rabbit sera (Sigma-Aldrich, St Louis, USA). The cells were grown at physiologically relevant +37°C suggested by ATCC, even though the optimal growth temperature for Bb would be +33°C (Hubálek *et al*., 1998). RBs were induced by re-suspending the cell pellets (1000 RCF, 15 min) in deionized sterile H_2O for 2 h at +37°C (Brorson and Brorson, 1998). The bleb forms were induced by reverting H_2O induced RBs in BSK-II medium at RT or at +37°C for 45–60 min. For TEM experiments, RBs were induced also in BSK-II medium with 10% human serum (Sigma-Aldrich) without BSA and rabbit serum, at 4 days incubation. Methanol fixing of the cells (1000 RCF, 15 min) was done with ice cold 100% methanol at -20°C for at least 20 min. Doxycycline (Hexal Ag, Holzkirchen, Germany) treatment of 100 µg/ml for 24 h, or 200 µg/ml for 48 h in the western blots, was utilized to induce the outer cell wall damage on Bb cells (Kersten *et al*., 1995; Meriläinen's manuscript, 2014). Doxycycline treated cells were used as controls.

3.2 Confocal microscopy

Bb spirochetes, 2 h H_2O RBs, biofilms and blebs were examined by confocal microscopy to study the distribution of DNA, lipids and polysaccharides. Methanol fixed cells were utilized as controls since methanol fixing creates holes in the membranes allowing the dyes to enter the cells. Doxycycline treated cells were included as controls for outer membrane damage. In addition, immunolabeling of flagellin was performed to check if flagella are conserved in the RB form.

3.2.1 Fluorescent staining of the pleomorphic forms of *B. burgdorferi*

Ethidium bromide (EtBr, Sigma Aldrich) and propidium iodide (PI, Sigma Aldrich) were used for staining double stranded DNA. Both EtBr, 0.025 mg/ml in PBS, and PI, 5 mg/ml in PBS, were utilized as 1:50 or 1:100 dilution. Live cells stained immediately upon adding the DNA dyes, but methanol fixed samples were incubated with the dyes for 10 min at RT. Lipids were stained with 1:100 dilution of 1 M Nile Red in 70% EtOH (72485 Sigma

Aldrich) and 1:2000 dilution of 1 mg/ml boron-dipyrromethene (Bodipy, 493/503) in DMSO (Molecular Probes, Eugene, USA). For both dyes the stock solutions were in PBS. Cells were incubated with either Nile Red or Bodipy for 1 h at +37°C, followed by a wash with PBS. N-acetyl glucosamines (GluNAcs) were stained with 1:100 dilution of 1 mg/ml wheat germ agglutinin (WGA-555, w32464, Molecular Probes) for 30 min at RT. Glycogen was stained with iodine solution containing 1% I_2 (Riedel-de Haën, Seelze, Germany) and 2% KI (Sigma Aldrich) in H_2O for 1 h at RT whereas collagen was stained with 1% Acid Fuchsin (84600, Fluka, Buchs, Switzerland). Acid Fuchsin and iodine solution dyes were only used for fixed cells. The dilutions of the dyes were made in BSK-II medium for the living cells and in PBS for the fixed ones. The living cells were washed with BSK-II medium (centrifuged at 1000 RCF for 15 min) and methanol fixed cells with PBS (at 15700 RCF for 1-2 min). Fixed samples were mounted with Prolong Gold medium containing DAPI (4', 6-diamidino-2-phenylindole, Molecular Probes).

3.2.2 Immunolabeling with flagellar antibody p41

Immunolabeling of flagella in Bb spirochetes and RBs was carried out to examine the organization of the flagella in RBs. Spirochetes and 2 h H_2O RBs, $20x10^6$ cells per sample, were fixed with ice cold methanol for a minimum of 20 min at -20°C, followed by a wash with PBS. Centrifugation was performed at 1000 RCF for 15 min with living cells and at 9300 RCF for 5 min with the fixed cells. Permeabilization was performed with Triton solution containing 0.1% Triton, 0.1% bovine serum albumin (BSA) and 0.01% NaN_3 in PBS with rocking for 15 min. The samples were incubated with 1:50 dilution of mouse anti-*Borrelia* p41 flagellin antibody (IgG2a, Acris GmbH, Herford, Germany) in Triton solution for 1 h with rocking. After a Triton solution wash followed the addition of 1:200 dilution of the secondary antibody goat anti-mouse IgG antibody conjugated with Alexa 488 (Invitrogen Carlsbad, USA, 2 mg/ml) in Triton solution for 30 min with rocking. Two washes with PBS preceded mounting with Prolong Gold.

3.2.3 Confocal imaging and image processing

Imaging of the fluorescent samples was performed with an Olympus microscope IX81 with a FluoView-1000 confocal setup, 60X objective, 488 or 546 laser and Differential Interference Contrast (DIC). Each staining was repeated at least twice. Image processing

was carried out with an open source program ImageJ (Rasband, NIH, USA). Brightness and contrast were optimized and uneven illumination was corrected with Pseudo correction in the DIC images when needed. Background noise in the fluorescent images was decreased by Gaussian blur (radius 1).

3.3 Transmission electron microscopy (TEM)

Electron microscopy was utilized to unravel structural details of the membranes in RBs and to examine the coiling of spirochetes into RBs. Negative staining was carried out to illustrate the general structure of the forms. Thin sections demonstrated a more detailed insight to the structure where even the distribution of the flagella could be observed. Imaging was performed with JEOL-JEM 1400 transmission electron microscope (TEM).

3.3.1 Negative staining with PTA

Negative staining was performed with phosphotungstic acid (PTA). Methanol fixed bacteria, spirochetes and 2 h H_2O induced RBs, were pipetted on Formvar carbon coated 200Mesh copper grids (FCF-200-Cu, Electron Microscopy Sciences, Hatfield, USA). First methanol was removed from the Bb samples with three H_2O washes (15700 RCF, 2 min). Cells were incubated on the grids for 1 min. Incubation with PTA, for 1 min, was followed by several quick washes with H_2O. All the solutions were filtered to remove impurities. The grids were air dried and kept in a desiccator prior to imaging.

3.3.2 Epon embedded thin sections

Bb spirochetes, blebs, and 4 d human serum as well as 2 h H_2O RBs were prepared as duplicates for TEM thin sectioning. The cell amount was $1x10^9$ for each sample. All samples were centrifuged at 2400 RCF for 15 min and fixed with 2.5% glutaraldehyde in 0.1 M phosphate buffer for 10 min at RT. Finally the fixed cells were transferred into eppendorf tubes, centrifuged 2800 RCF for 30 min and stored at +4°C for epon embedding.

The samples were centrifuged with a swing-out centrifuge (Heraeus Megafuge 1.0R, BS 4402/A) at 6240 RCF for 5 min at RT and washed three times with fresh 0.1 M phosphate buffer and twice with H_2O, 10 min per wash. Liquid 2.5% agarose, +37°C, was added to

air dried pellets. Then the samples were spun down for 2 min at 6240 RCF. The pellets were transferred into glass jars, containing 1% osmium tetroxide for 30 min at RT. Three 10 min washes with H_2O followed preceding the incubation with 1% uranyl acetate for 30 min at RT. Afterwards three washes with H_2O were repeated. Dehydration of the samples was performed with a rising acetone concentration series of 30%, 50%, 70% and to conclude twice with 100% acetone, 10 min per solution. Embedding with embedding resin medium started with 1:1 epon-acetone solution for 45 min at RT. Followed by 100% epon (Taab Laboratories Equipment Ltd, UK) at RT overnight (o/n). Afterwards, the cells were transferred into pre-marked molds with 100% epon. The samples were first incubated at +40°C for 2 h and then at +60°C for 24 h. The blocks were thin sectioned at the Biocenter Oulu Electron Microscopy Core Facility.

3.3.3 Analysis of the round body TEM images

TEM images of RBs induced by 2 h H_2O and 4 d human serum were analyzed by comparing the amount of RBs containing "normal" against swollen protoplasmic cylinders. Protoplasmic cylinders that had a diameter of approximately 200 nm were considered normal. If the diameter appeared to be much larger, above 500 nm, the protoplasmic cylinder was counted as swollen. An amount of 171 RBs from H_2O induced and 212 from human serum induced RBs were analyzed.

3.4 Surface-to-volume ratios of spirochetes and RBs

The surface to volume ratios of spirochetes and RBs were examined to create a more profound picture of the changes occurring during the form switching. RBs have a diameter of 2.8 ± 0.46 µm, measured from confocal images (DIC). In TEM images the diameter was observed to be slightly smaller, approximately 2.4 µm (Meriläinen's manuscript, 2014). Generally, spirochetes are described to be 10–30 µm in length and 0.18–0.25 µm in diameter (Burgdorfer *et al*., 1982). Here the surface area and volume of spirochetes and RBs were estimated by modelling these forms as cylinders and balls respectively. See the calculations in Results.

3.5 Comparison of spirochete and RB protein profiles by 2D PAGE

Two dimensional polyacrylamide gel electrophoresis (2D PAGE) was performed for the examination of differences between the protein profiles of Bb B31 spirochetes and 2 h H_2O RBs. Samples containing 1-2x10^9 cells each were centrifuged at 2400 RCF for 15 min and stored at -20°C. Lysing was carried out by 8 rounds of 15 s sonication, in a mixture containing 910 µl of 1x ZOOM 2D Protein Solubilizer 2 (Invitrogen), 3 µl 1 M Tris base (Sigma Aldrich), 10 µl 2 M DL-dithiothreitol (DTT, Sigma Aldrich) and 10 µl 10X Protease inhibitor single-use cocktail (EDTA-Free) pH 8.4 (Thermo Scientific, Rockford, USA). The lysates were first incubated on a shaker for 15 min at RT then treated with 5 µl 99% N, N-dimethylacrylamide (DMA, Sigma Aldrich) for 30 min with shaking at RT. Finally, the lysates were centrifuged at 15800 RCF for 20 min at +4°C with 10 µl 2 M DTT. Then the samples were homogenized with QIAShredder microcentrifuge tube (Qiagen, Hilden Germany) centrifuged at 16000 RCF for 1 min. The protein concentration was determined by Nanodrop ND-1000 spectrophotometer (Thermo Scientific, Wilmington, USA) and the lysed samples were stored at +4°C. Rehydration solution, utilized for rehydrating the immobilized pH gradient (IPG) strips, consisted of 143 µl 1x ZOOM 2D Protein Solubilizer 2, 0.7 µl 2M DTT, 0.8 µl Carrier ampholytes pH 3–10 (Novex Life Technologies, Carlsbad USA) and 0.5 µl 0.2% bromophenol blue in EtOH (Merck, Darmstadt, Germany). IPG strips (broad range pH 3–10, Novex Life Technologies) were equilibrated for 1 h at RT with the lysed cell sample (36 µg protein) in 155 µl rehydration buffer. Isoelectric focusing (IEF) was performed with a stepwise program: 175 V for 15 min, 1500 V for 45 min and 2000 V for 45 min. Subsequently, the strips were equilibrated for gel electrophoresis with 1x Sample reducing agent (Invitrogen) and 125 mM iodoacetamide (Sigma Aldrich) both in 1X NuPAGE LDS sample buffer (Invitrogen). In both solutions the samples were incubated for 15 min rocking at RT. NuPAGE Novex 4–12% Bis-Tris ZOOM gels were used for gel electrophoresis. To restrain the strip in place in the gel 0.5% agarose in Tris buffer (124 mM Tris, 960 mM glycine, 17.3 mM SDS) was utilized. Gel electrophoresis was performed in 1X NuPAGE 2-[N-morpholino]ethanesulfonic acid (MES) SDS Running buffer (Invitrogen), with 0.5 ml NuPAGE Antioxidant (Invitrogen) in the upper chamber, at 200 V for 45 min. Mark12 unstained standard (Invitrogen) was utilized as the molecular weight standard. The gels were stained with SilverQuest SilverStaining kit (Invitrogen) according to the

manufacturer's instructions except the sensitizing and staining times were doubled (20 and 30 min respectively). The gels were then fixed for 40 min or o/n at RT. Images of the gels were obtained with QuantityOne Chemdoc XRS (BIO-RAD).

An open source software, Flicker (Lemkin *et al*., 2005), was utilized for the intensity measurements of the protein spots on the gels. Corresponding protein spots were chosen from spirochete and RB gels. The experiments were repeated three times for both forms. The intensity values were normalized with a spot from the molecular weight standard. Mean values for each spot were compared to analyze whether the protein expression in RBs was diminished or increased compared to spirochetes (see Table 2).

3.6 Antigenicity of spirochetes and RBs to Lyme disease patient sera

Western blots of whole cell lysates from Bb spirochetes and 2 h H_2O RBs were probed with Lyme disease patient sera to examine the antigenicity of the pleomorphic forms. Cells treated with doxycycline, 200 µg/ml for 48 h, were used as a control. At first, cells were collected by centrifugation at 2400 RCF for 15 min and re-suspended in PBS. The samples were boiled for 10 min, followed by addition of 2X SDS reducing loading buffer (5 ml of 0.5 M Tris HCl pH 6.8, 8 ml of 10% SDS, 8 ml of 50% glycerol, 0.2% bromophenol blue, 2 ml of 2-β-mercaptoethanol in 16 ml H_2O) and 5 min boiling. Protein concentration was measured by Nanodrop ND-1000 spectrophotometer (Thermo Scientific). Protein amount per well was 20 µg and the volume was adjusted to 30 µl with 2X SDS reducing loading buffer. The samples were boiled for 5 min before addition to 1.5 mm thick 4%–12% SDS PAGE gels. High and low SDS Laemmli PAGE system (Sigma-Aldrich) molecular weight standards were added on the gels. The gels ran at 100 V for 10–20 min, followed by 180 V for 40 min, with BIO-RAD equipment.

The proteins were transferred to nitrocellulose membranes in blotting buffer containing 25 mM Tris pH 8.3, (Sigma-Aldrich), 192 mM glycine, (Sigma-Aldrich), and 20 % methanol (Fluka) for 1 h at 100 V. The membranes were stained with 0.2% Ponceus red in order to mark the molecular weight standards. Blocking was performed with 5% non-fat milk 1% in tris-buffered saline (TBS, Medicago AB, Uppsala, Sweden) - 0.2% Tween20 (Sigma-Aldrich) either for 1 h at RT or o/n at +4°C with rocking. Immunolabeling was preceded by three washes with washing buffer, 1X TBS-0.2% Tween20 (TBS-T), 5 min per wash.

The membranes were incubated with 1:100 human serum in TBS-T for 1 h at RT, followed by three 5 min washes with TBS-T. Seven pre-screened positive and three negative sera from the Federal Institute for Drug and Medical Devices, Germany were used (ethical approval number 95.10-5661-7066). The positive sera were chosen due to earlier ELISA studies that had shown differences in the antigenicity between spirochetes and RBs (Thammasri's manuscript, 2014). Secondary antibody incubation was carried out with 1:500 dilution of anti-human polyclonal IgG Fc-antibody (Novus Biologicals, Cambridge, UK) in alkaline phosphate assay buffer (APA, containing 0.1 M Trizma, 0.1 M NaCl and 5 mM MgCl, Sigma-Aldrich, pH 9.5) for 1 h at RT. Three washes were repeated as before and the membranes incubated for 5 min in APA buffer. Colorimetric reaction was conducted for 10–20 min with nitro-blue tetrazolium and 5-bromo-4-chloro-3'-indolyphosphate (NBT, Promega, Madison, USA, and BCIP, Sigma-Aldrich) in APA buffer. The reaction was stopped with H_2O, and the dry membranes were imaged with Chemdoc XRS System. The protein band intensities were analyzed with ImageJ software.

4 Results

4.1 Structural differences in the pleomorphic forms observed by confocal microscopy

Various morphological traits of spirochetes, blebs, biofilms and 2 h H_2O RB forms of Bb were stained with fluorescent dyes and observed with confocal microscopy (Figure 2). The aim was to discover specific morphological traits specific for each pleomorphic form. DIC images demonstrate the amount of Bb cells and illustrate how deep the dyes penetrate in the cells when compared to the fluorescent images. Doxycycline treated cells served as a control for damaged cells. Methanol fixed cells were utilized as controls for the staining, as methanol creates holes to the membranes allowing the dyes to enter the cells.

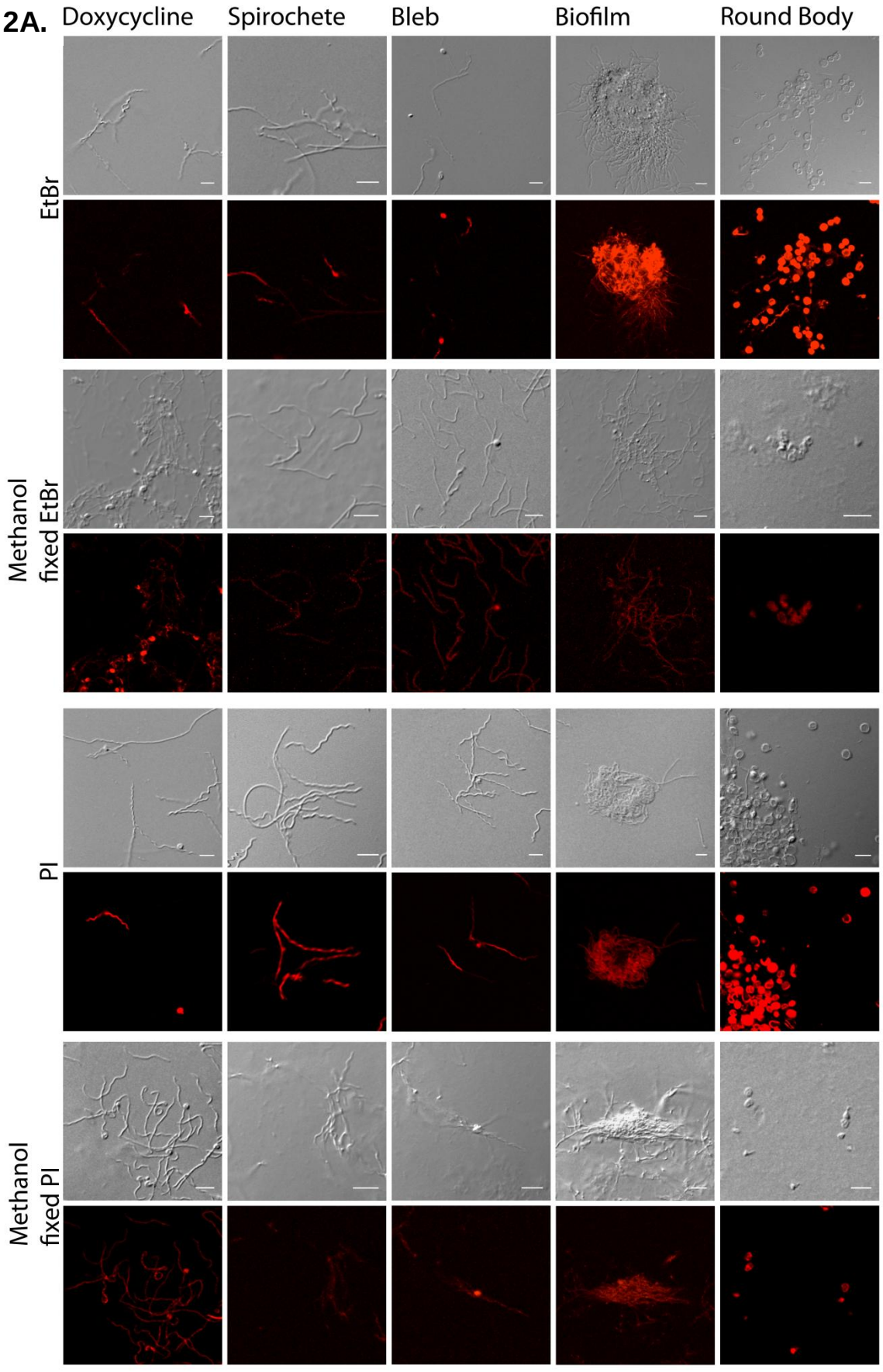
2A.
Doxycycline
Spirochete
Bleb
Biofilm
Round Body
EtBr
Methanol fixed EtBr
PI
Methanol fixed PI

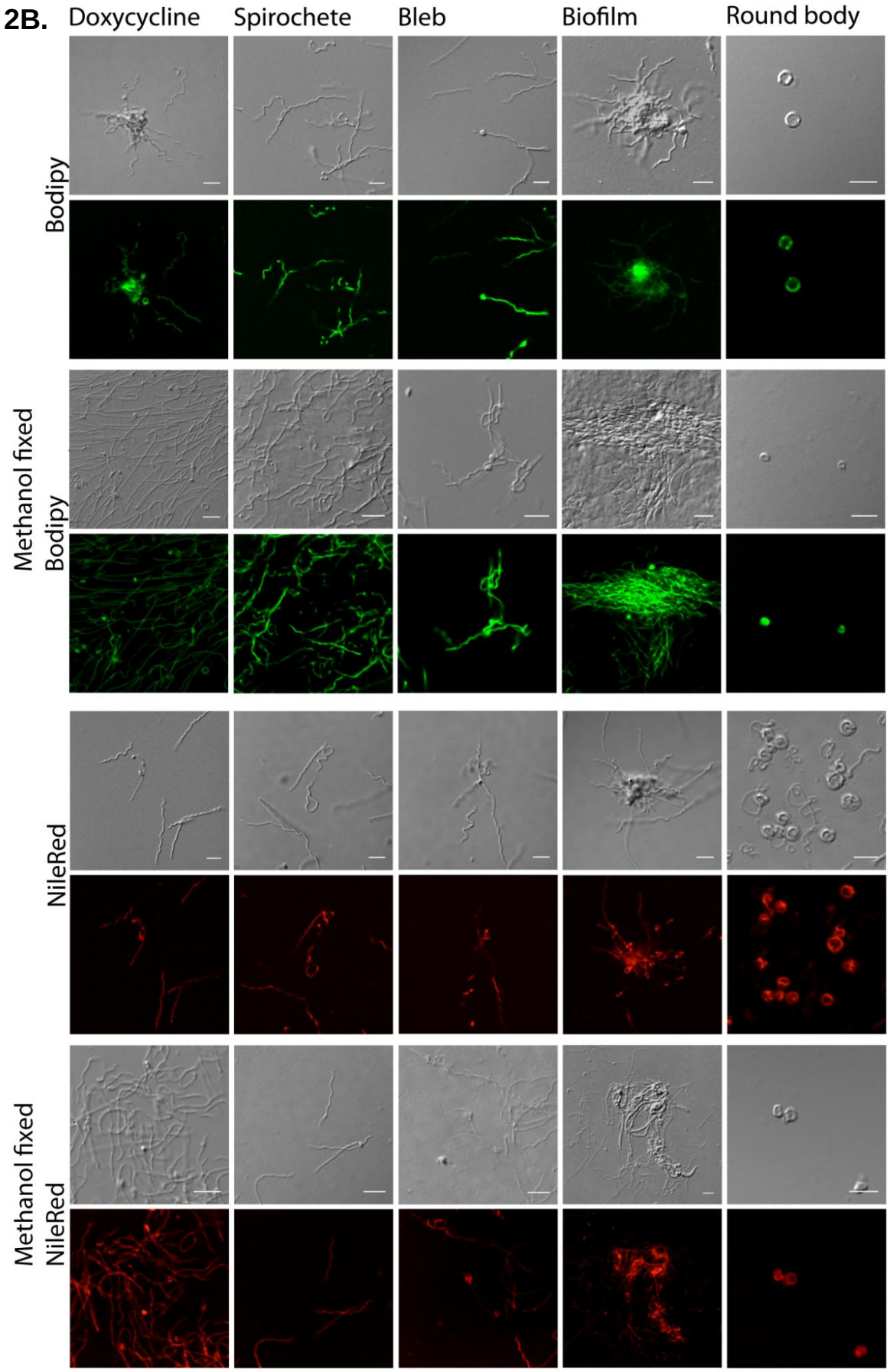
2B.
Doxycycline
Spirochete
Bleb
Biofilm
Round body
Bodipy
Methanol fixed Bodipy
NileRed
Methanol fixed NileRed

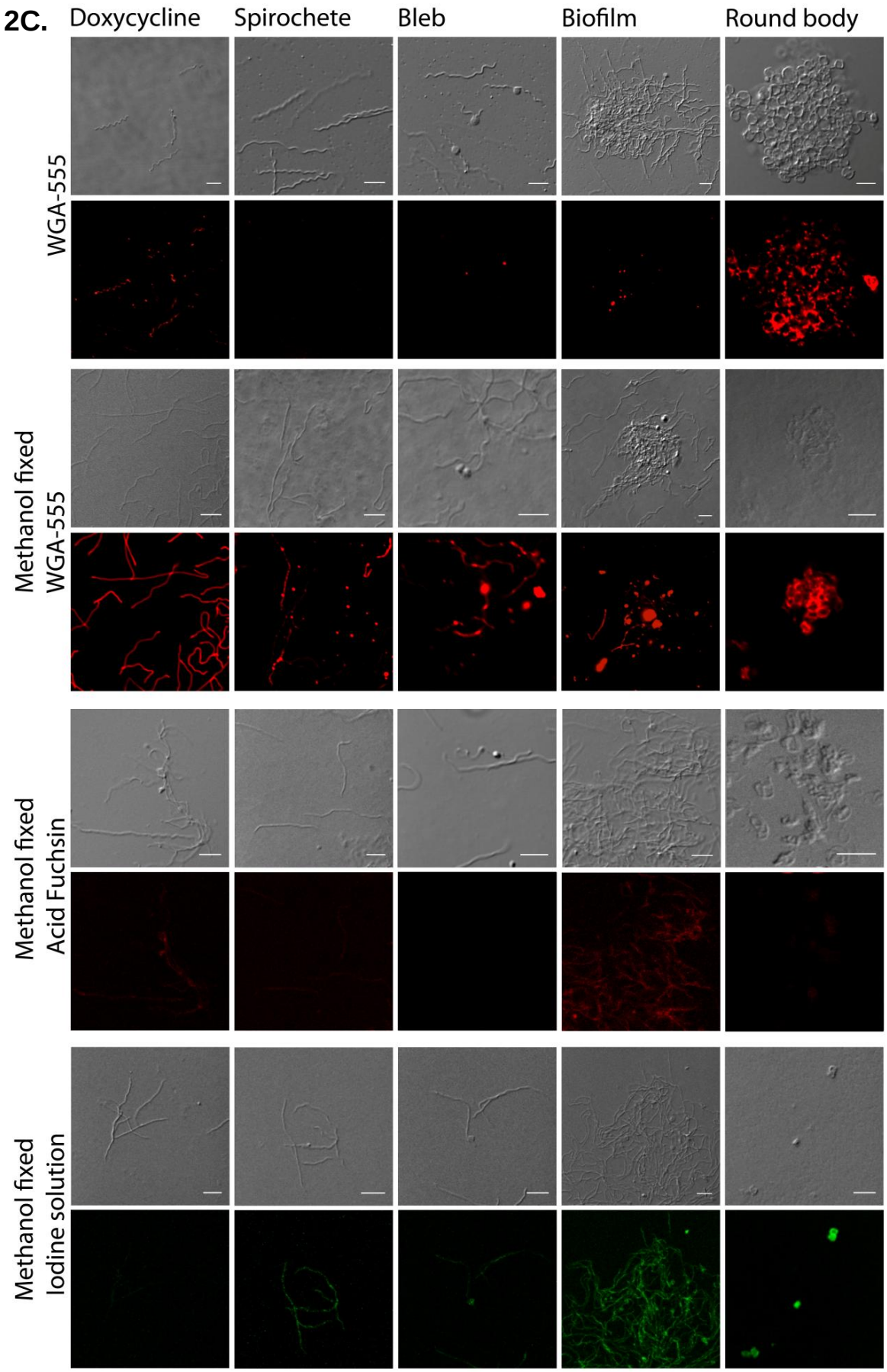
2C.
Doxycycline
Spirochete
Bleb
Biofilm
Round body
WGA-555
Methanol fixed
WGA-555
Methanol fixed
Acid Fuchsin
Methanol fixed
Iodine solution

Figure 2: Structural traits differ in the pleomorphic forms of Bb. Representative images of doxycycline treated (first column) and pleomorphic forms of Bb strain B31 stained with DNA (**A**), lipid (**B**) and polysaccharide and collagen (**C**) dyes. Bleb form is also included as an intermediate step between spirochetes and RBs.. RBs were induced by 2 h H_2O treatment. DNA was dyed with PI and EtBr, lipids with Bodipy and Nile Red, GluNAcs with WGA, collagen with Acid Fuchsin, and glycogen with iodine solution. DIC and confocal images are provided from living and methanol fixed samples. Scale bar 5 µm. Only methanol fixed samples were used for Acid Fuchsin and iodine solution staining.

Staining with EtBr and PI dyes confirmed that all pleomorphic forms of Bb as well as blebs contain DNA, seen as red in the Figure 2A. Both PI and EtBr entered living cells in addition to the methanol fixed cells. However, all of the living cells were not stained, as indicated by the DIC images. Even the cell membrane damaged doxycycline treated cells were not all stained in the living samples (Figure 2A, EtBr and PI first column on the left). Movement of the living cells containing the DNA dyes was observed, but after a short period of time these cells seemed to become non-motile. RBs (Figure 2A, the last column on the right) seemed to be easily accessible to the DNA dyes because they stained brightly in the live samples. Bleb structures contained DNA as well (Figure 2A, the column in the middle). In the methanol fixed control samples, all cells were stained in all pleomorphic forms, although the staining seemed to be quite weak. DNA was also ubiquitously present in the doxycycline treated cells (Figure 2A, the first column on the left).

The lipid composition seemed to be conserved in all pleomorphic forms as well as in blebs when stained with the lipid dyes Bodipy and NileRed (Figure 2B). Bodipy dye detected neutral lipids in all forms of Bb, seen as green in the upper part of the Figure 2B. Similarly NileRed, commonly used for staining intracellular vesicles (Greenspan *et al*., 1985), was detected in all forms. Nile Red is seen as red in the lower part of the Figure 2B. In addition, in the RBs (Figure 2B, the last column on the right) the lipid dyes seemed to penetrate further inside the cells in the methanol fixed samples.

WGA is a lectin specific for the GluNAc residues of bacterial peptidoglycan. WGA seemed to surround RBs, seen as red (Figure 2C, the last column on the right). Live blebs were not stained (Figure 2C, the column in the middle). GluNAcs seemed to be accessible also in the doxycycline treated controls (Figure 2C, the first column on the left). In the methanol fixed samples WGA entered the cells and peptidoglycan was stained in all forms. Some background staining was observed because BSK-II media contains GluNAcs. Collagen stained with Acid Fuchsin in the methanol fixed samples was exclusively

observed in biofilms, seen as red (Figure 2C, the second column from the right). The doxycycline treated sample seemed to include a biofilm structure and was thereby stained with Acid Fuchsin (Figure 2C, the first column from the left). Iodine solution was used to stain glycogen in methanol fixed samples. Glycogen was observed in all pleomorphic forms as well as in blebs, seen as green, but seemed to be absent in the doxycycline treated control cells.

4.2 An insight to RB formation

A fundamental aspect of pleomorphism is the ability to revert back to the parental form. In the 2 h H_2O induced RBs the protoplasmic cylinder maintains its shape while coiling inside the enlarging periplasmic space (Figure 3A). Thereby the double membrane structure seems to be conserved in RBs. In addition, the flagella were still present next to the protoplasmic cylinder in RB form. The presence of flagella was confirmed with immunolabeling (Figure 4).

4.2.1 Coiling of spirochetes into RBs step-by-step

The formation of RBs from spirochetes (Figure 3A1) seems to begin with a large bleb formation in the outer membrane (Figure 3A2). This bleb enlarges and the protoplasmic cylinder starts to coil inside (Figure 3A3-3A4). Periplasmic space between the inner and outer membranes grows (indicated by arrows in Figure 3A). The coiling of the protoplasmic cylinder inside RBs is demonstrated in Figure 3B from different angles. The protoplasmic cylinder does not seem to occupy the whole periplasmic space (Figure 3B3), but coil in as large loops as possible along the outer membrane (Figure 3B2). In Figure 3B1, a part of the spirochete is protruding outside the RB as a tail.

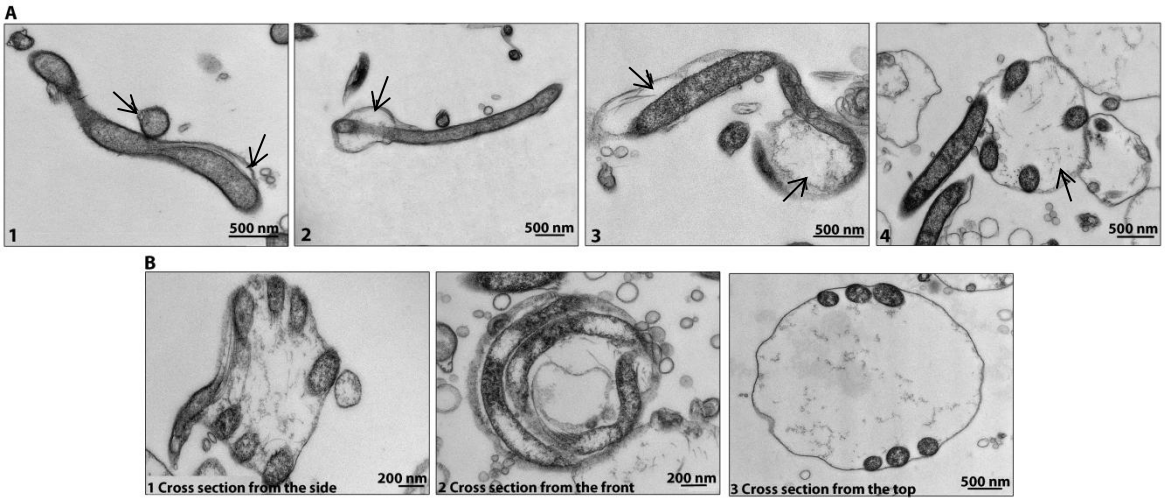

Figure 3: Formation and structure of RBs. Steps of RB formation from Bb B31 spirochetes in medium containing 10% human serum (panel A 1–4) shown with TEM micrographs. Longitudinal and transversal spirochete cross sections are illustrated in A1 (in BSK-II medium). The protoplasmic cylinder is approximately 200 nm in diameter. Periplasmic space between the inner and outer membrane is shown with arrows. Images A2-A4 demonstrate the blebbing of the outer membrane and how the protoplasmic cylinder coils into the enlarged periplasmic space. In panel B, the result of folding of the protoplasmic cylinder inside the periplasmic space is displayed by images of RB cross sections from different angles (B1-B3).

4.2.2 Surface-area-to-volume ratio diminishes greatly during the formation of RBs

Spirochetes undergo a notable change in shape when forming RBs (see calculations 1–6 below). For example, the surface-area-to-volume ratio changes dramatically as spirochetes (A/V = 20) form RBs (A/V = 2.1). These results are merely approximations estimated by modelling spirochetes as cylinders and RBs as balls. However, they do emphasis the vast changes in volume and surface area that must happen when the bacteria change their conformation from one form to another.

$$A_{\text{Round body}} = 4\pi r^2 = 4\pi\left(\frac{2.8\ \mu m}{2}\right)^2 = 24.6\ \mu m^2 \quad (1)$$

$$V_{\text{Round body}} = \frac{4}{3}\pi\left(\frac{2.8\ \mu m}{2}\right)^3 = 11.5\ \mu m^3 \quad (2)$$

$$\frac{A_{\text{Round body}}}{V_{\text{Round body}}} = \frac{24.6}{11.5} = 2.1 \quad (3)$$

$$A_{\text{Spirochete}} = 2\pi rh + 2\pi r^2 = 2\pi(rh + r^2) = 2\pi\left(\frac{0.2\ \mu m}{2} \times 20\ \mu m + \left(\frac{0.2\ \mu m}{2}\right)^2\right) = 12.6\ \mu m^2 \quad (4)$$

$$V_{\text{Spirochete}} = \pi r^2 h = \pi\left(\frac{0.2\ \mu m}{2}\right)^2 \times 20\ \mu m = 0.63\ \mu m^3 \quad (5)$$

$$\frac{A_{\text{Spirochete}}}{V_{\text{Spirochete}}} = \frac{12.6}{0.63} = 20 \quad (6)$$

4.3 Flagella are conserved in RBs

Flagella are located in the periplasmic space in Bb spirochete form. They have been observed to reside close to the outer membrane, between the peptidoglycan layer and the outer membrane (Johnson *et al*., 1984; Kudryashev *et al*., 2009). Flagella are seen as green in spirochetes and RBs with the anti-*Borrelia* flagellar antibody p41 in Figure 4. Since the green fluorescence is not seen uniformly throughout the RBs, flagella do not seem to be located all over the enlarged periplasmic space (Figure 4B, DIC and fluorescent images). They seem to rather follow the coils of the folded protoplasmic cylinder. Also the TEM images of RBs (Figure 4B) support this observation, since the flagella seem to be located right next to the protoplasmic cylinder. The distribution of flagella in spirochetes in the periplasmic space is shown in Figure 4A TEM images.

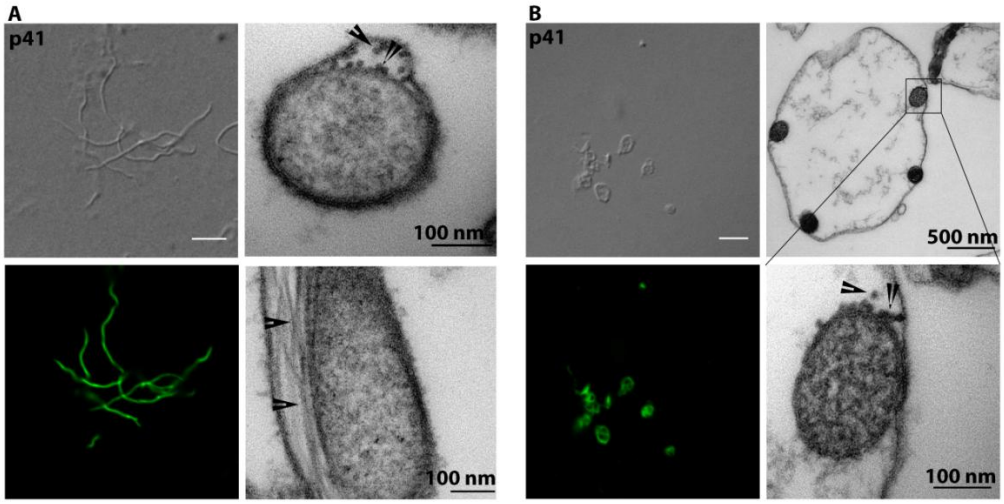

Figure 4: Flagella are conserved in the RB form. Bb B31 spirochetes (A) and 2 h H_2O RBs (B) labeled with flagellar antibody p41 shown as green fluorescent and DIC confocal images. TEM images are also provided. Arrows point out the location of flagella in the periplasmic space. Scale bar in the confocal images is 5 µm.

4.4 Swelling of protoplasmic cylinders in RBs induced by human serum

Incubation of Bb in human serum for 4 d triggered RB formation. RBs appeared to have similar structure as the H_2O induced RBs, for example the two lipid bilayers were undamaged. However, in the human serum induced RB TEM micrographs, a large portion of RBs were detected to contain significantly larger protoplasmic cylinders than the approximate 200 nm wide "normal" protoplasmic cylinder (Figure 5, Table 2). In Figure 5,

swollen protoplasmic cylinders are marked with SP and “normal” protoplasmic cylinders are indicated by white stars (*). Both, the inner and outer, membranes seemed to be undamaged in the RBs with swollen protoplasmic cylinders (Figure 5 images D and F, arrows). This phenomenon seemed to be more common in human serum induced RBs than in H_2O induced RBs since almost a third of the RBs had swollen protoplasmic cylinders in the human serum samples compared to a minor 4% in H_2O samples (Table 2).

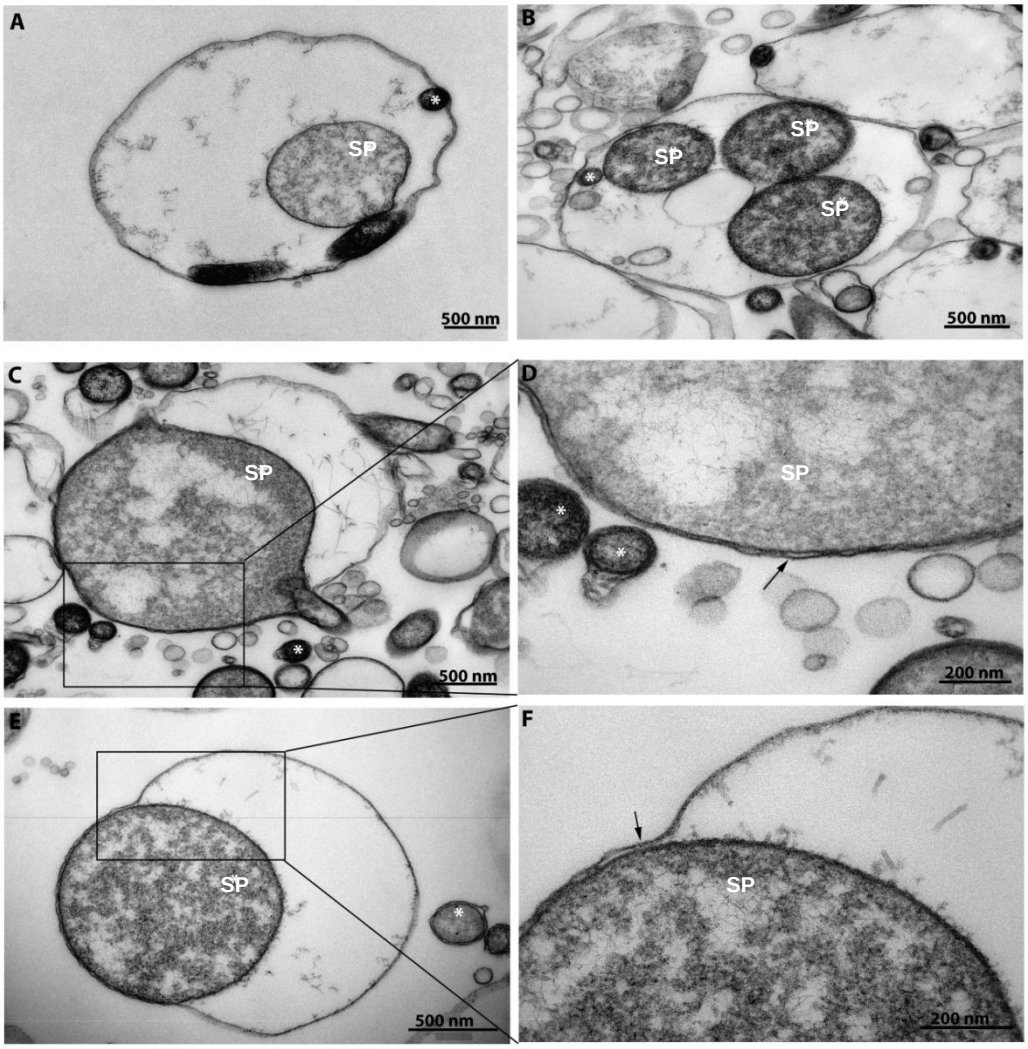

Figure 5: Swelling of the protoplasmic cylinders in RBs induced by human serum. Swollen protoplasmic cylinders of Bb B31 RBs induced for 4 d in human serum are marked with SP in the TEM micrographs. To emphasize the size difference of the protoplasmic cylinders, the “normal” protoplasmic cylinders of neighboring spirochete cross sections are marked with white stars. Swollen protoplasmic cylinders have a diameter of >500 nm whereas “normal” ones approximately 200 nm. Intact double membrane pin pointed with arrows in the zoomed in images D and F.

Table 2: Human serum and H_2O induced RBs with swollen protoplasmic cylinders. RBs containing "normal" versus swollen protoplasmic cylinders counted from TEM micrographs. Normal protoplasmic cylinders have a diameter of 200 nm whereas in swollen ones the diameter is above 500 nm. The swelling of the protoplasmic cylinders was analysed in the 2 h H_2O RBs and 4 d human serum induced RBs.

	"Normal" protoplasmic cylinders	%	Swollen protoplasmic cylinders	%	Total of RBs counted
2 h H_2O RBs	164	96%	7	4%	171
4 d HS RBs	153	72%	59	28%	212

4.5 Increased vesicle formation induced by human serum

A large amount of vesicles was observed in the TEM thin section images of 4 d human serum induced RBs (see arrows in Figure 6). Beading of the outer membrane was equally observed in substantial amount (Figure 6, images A-F). Vesicle formation is illustrated in blebs (Figure 6, images A-B) and RBs (Figure 6, images C-F and I-J). The budding vesicles were of different size ranging from about 50 nm up to 200 nm. The smallest vesicles formed a chain of pearls kind of structures (Figure 6, image E). Some spirochetes seemed to be wrapped by vesicles (Figure 6 images G and H). Few internal vesicles were also observed in the RBs (Figure 6 images I and J). The vesicle formation did not seem to be as intensive in 2 h H_2O induced RB samples.

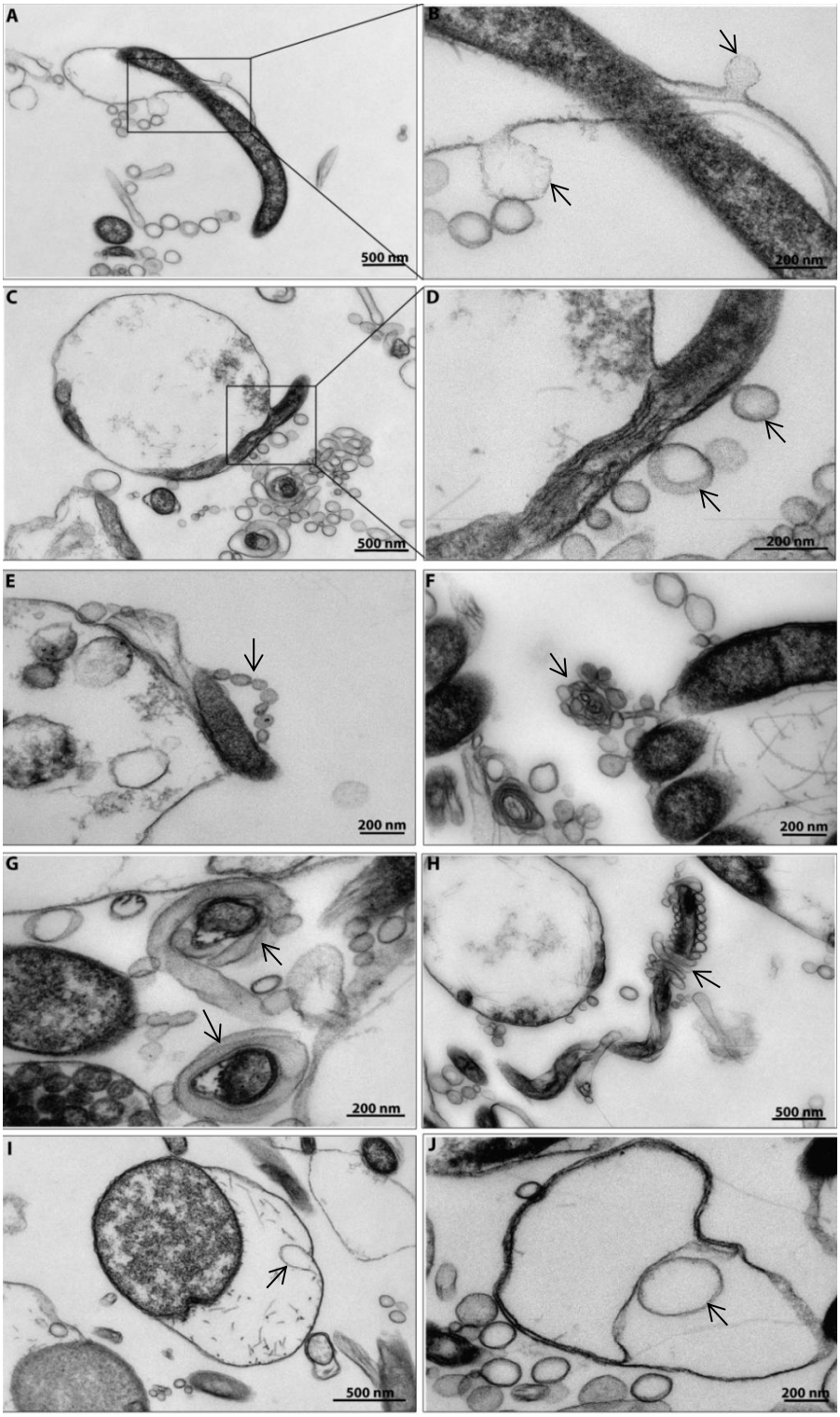

Figure 6: Stressful conditions created by human serum increased vesicle formation. Representative images of various vesicle types observed in the 4 d human serum induced Bb B31 cells. Vesicles indicated by arrows in TEM micrographs, images A-J. Vesicle formation from the outer membrane of a bleb (A and B) and a round body (C and D) with the vesicle size of approximately 100-200 nm (A-D). A chain of pearls like vesicle formation (diameter approximately 50 nm) demonstrated in image E. Images G and H illustrate vesicles wrapping around spirochetes. Possible source of the wrapping vesicles is suggested in image F. Vesicle formation inside round bodies from the inner membrane (I and J).

4.6 The expression of several 15–40 kDa proteins is higher in RBs than in spirochetes

Proteins from whole cell lysates from Bb B31 spirochetes and 2 h H_2O RBs were separated first according to their isoelectric point, pI (pH gradient 3–10), and then based on their molecular weight (Figure 7). Differences in the protein expression were studied between the forms to support the hypothesis that the forms represent pleomorphism. Out of the measured 77 protein spots, those with relative intensity difference greater than 25% between spirochetes and RBs are displayed in the Table 3 and Figure 7. The intensity values are an average of three 2D gels for both spirochetes and RBs. As seen in Figure 7, the protein spots of interest are mainly located at molecular weight areas 14–35 kDa (spots 12–26) and 200 kDa (spots 1–7). The expression of 15 proteins was elevated in RBs whereas for 12 proteins the expression was diminished in RBs compared to spirochetes (Table 3). The proteins whose expression was elevated in the RB form were between the molecular weight range 15–40 kDa (Table 3). Interestingly, a 21 kDa protein (protein spot 17) had a greater expression in spirochetes than in RBs. The greatest intensity difference, approximately 50 %, in the protein expression was observed in spots 3, 4, 14 and 21 (Figure 7, Table 3).

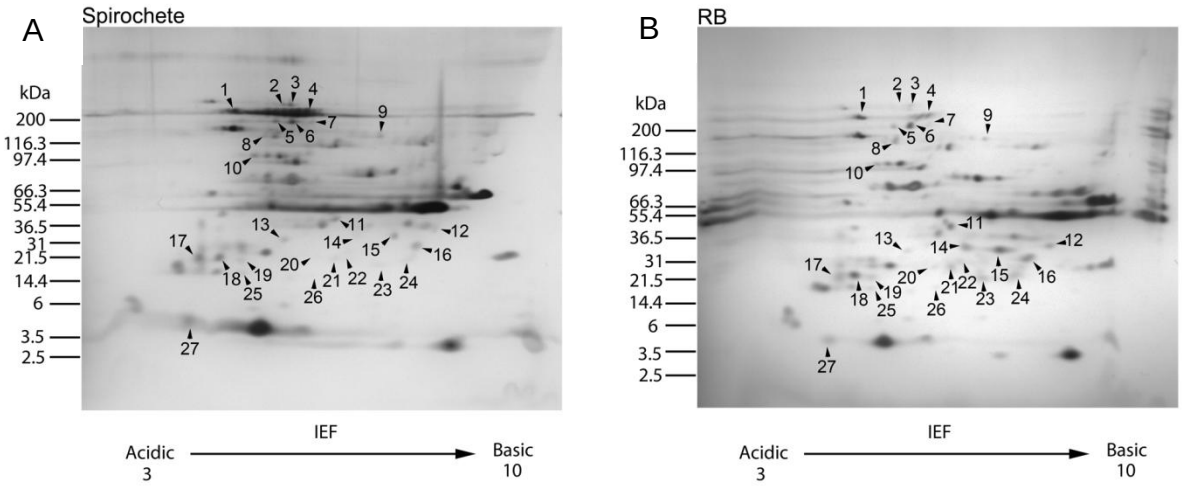

Figure 3: Distinctive protein profiles of spirochetes and RBs. Representative 2D PAGE gels from Bb B31 spirochete (A) and 2 h H_2O RB (B) whole cell lysates. Corresponding protein spots of interest with a relative intensity difference above 25% are marked (1–27) in both silver stained gels.

Table 3: Differences in the protein expression between Bb spirochetes and RBs. Corresponding protein spots (1-27) of spirochetes (S) and 2 h H_2O RBs were examined in 2D PAGE gels (N=3 for both spirochetes and RBs). Out of 77 analyzed protein spots, 27 spots with a relative intensity difference greater than 25% are displayed here. The increase (+) or decrease (-) of the protein expression in RBs versus spirochetes is demonstrated in the table.

Spot	~Mw (kDa)	S	RB	Difference (%)	Spot	~Mw (kDa)	S	RB	Difference (%)
1	>200	+	-	31.5	**15**	33	-	+	41.5
2	>200	+	-	45.2	**16**	31	-	+	27.7
3	>200	+	-	49.3	**17**	21	+	-	35.7
4	>200	+	-	58.8	**18**	21	-	+	39.9
5	200	+	-	47.5	**19**	21	-	+	34.0
6	200	+	-	26.2	**20**	27	-	+	33.9
7	200	+	-	37.6	**21**	27	-	+	49.9
8	120	+	-	27.5	**22**	27	-	+	42.2
9	160	+	-	34.9	**23**	18	-	+	38.4
10	97	+	-	33.4	**24**	18	-	+	35.4
11	40	-	+	36.5	**25**	15	-	+	29.7
12	33	-	+	32.6	**26**	15	-	+	33.7
13	33	-	+	26.6	**27**	4	+	-	28.7
14	33	-	+	51.6					

4.7 Spirochetes and RBs raise different protein-antibody reactions with Lyme disease patient sera

The antigenicity of spirochetes and 2 h H_2O RBs were compared by western blots of Bb B31 whole cell lysates probed with human serum from Lyme disease patients (Figure 8). Seven positive and three negative sera were examined. The antigenicity of RBs was stronger than the antigenicity of the doxycycline (D) treated membrane damaged control cells (Figure 8). The serum antibodies seemed to bear distinct responses to spirochetes and RBs since the band intensities were not equal in western blots (Figure 8). Many bands were observed to have a higher intensity in RBs (Table 4). For example, the bands 70 kDa, 65 kDa, 56 kDa and 34 kDa were clearly observed to have a stronger intensity in RBs (Table 4). The band of a molecular weight 39 kDa was exclusively observed in RBs with one single serum. The difference in the protein band intensities between spirochetes and RBs was considered significant if it was at least 25%. On the other hand, the antibodies differed from serum to serum and thereby each serum gave a unique response to the bacterial antigens hence all of the protein-antibody interactions were not seen ubiquitously in the membranes (Table 4, Protein bands present in sera).

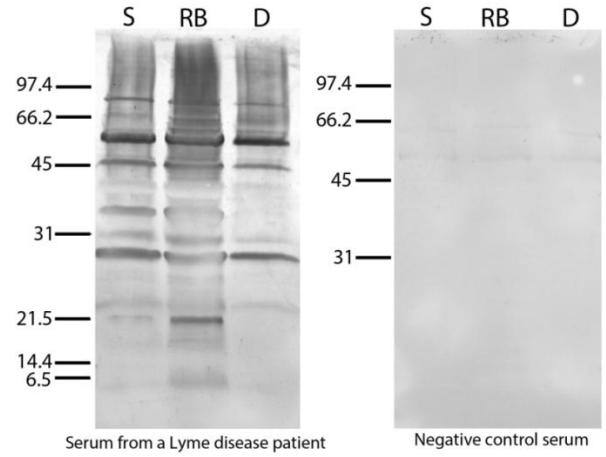

Figure 4: Immune reactivity of spirochetes and RBs. Representative images of western blots from Bb B31 spirochete (S), 2 h H_2O RB and 48 h 200 µg/ml doxycycline treated (D) whole cell lysates probed with human serum positive (on the left) and negative (on the right) for Lyme disease. The sera were diluted 1:100 and anti-human polyclonal IgG, 1:500, was utilized as the secondary antibody. The molecular weight markers are shown in kDa. Doxycycline treated cells were included in the gels as controls. Colorimetric staining with NBT and BCIP in APA buffer was utilized and analysis performed with ImageJ.

Table 4: Varying antibody responses to spirochetes and RBs. Protein band intensities compared between the whole cell lysates of Bb spirochetes (S) and 2 h H_2O RBs measured from western blot membranes probed with seven Lyme disease patient sera. The table displays the number of positive sera for a certain band and whether the intensity of the band was stronger in spirochetes or RBs. The intensity difference was considered relevant only when it was at least 25%.

Mw (kDa)	Stronger band intensity Difference >25%		Protein band present in X/7 sera
	S	RB	
93	-	3	6/7
70	-	2	2/7
65	-	3	4/7
56	-	5	6/7
55	-	4	7/7
45	2	1	6/7
41	1	4	6/7
39	-	1	1/7
36	1	4	7/7
34	-	4	5/7
31	1	4	7/7
29	1	2	7/7
26	1	1	5/7
23	-	2	3/7
21	-	4	7/7
18	1	2	6/7
6	-	1	5/7

5 Discussion

5.1 Structural traits of the pleomorphic forms

Various structural traits of the pleomorphic Bb forms were examined by confocal microscopy. Double stranded DNA was detected in all forms of Bb, also in the doxycycline treated cells with damaged outer membranes. It is notable though that PI stains also RNA (Suzuki *et al*., 1997). Both EtBr and PI are DNA dyes that are usually used in live-dead analysis of bacterial cells (Sachsenmeier *et al*., 1992; Banerjee *et al*., 2014). The dyes are supposed to only enter in dead cells with injured cell membranes. However, it seems that the unique cell envelope of Bb allows these dyes to enter into the living cells (Figure 2A), even though not all of the cells become stained. In the end the dyes probably do kill the bacteria, since the live cells containing these dyes seemed to shortly become non-motile. All of the used DNA dyes: EtBr, PI, and DAPI, intercalate between the base pairs in double stranded DNA and become fluorescent there. The similar staining mechanism of PI, EtBr, and DAPI might explain why the fluorescence seemed to be so dim in the methanol fixed samples since DAPI, from the mounting medium, would compete of the binding sites (Figure 2A). Similarly, the intercalation of the dyes into DNA double strand might provide an explanation to the ceased movement of the living cells observed shortly after the staining with PI or EtBr, because the cells are likely to die after the covalent attachment of the dyes into DNA (Garland *et al*., 1980).

The lipid constitution of the pleomorphic forms of Bb seemed also to remain the same in all forms since the staining patterns of the lipid dyes Bodipy and Nile Red were similar in all forms (Figure 2B). Respectively, Al-Robaiy *et al*. (2010) observed no differences in the phospholipid composition of spirochetes and RBs with mass spectrometry. The conserved double membrane lipid structure was seen also in TEM images, which supports the staining results (Figure 3). Also, the lipid membrane structure seemed to be undamaged in live RBs since the lipid dyes penetrated deeper into the methanol fixed RBs (Figure 2B). However, since the doxycycline treated cells were also stained by these lipid dyes, it is probable that the dyes cannot point out changes in the lipid architecture of the membranes (Figure 2B). Nevertheless, it seems likely that the lipid composition of Bb is not responsible for the form switching (Al-Robaiy *et al*., 2010).

Individual identification of Bb RBs could be carried out by using lectins. The presence of peptidoglycan in all forms of Bb was demonstrated by WGA staining of methanol fixed cells, but only RBs were stained in the living samples (Figure 2C). WGA is a lectin dye that binds specifically to GluNAcs (Vancová *et al*., 2005). This would indicate that peptidoglycan becomes exposed on the surface of the RBs (Figure 2C). The work of Sterba *et al*. (2008) supports the absence of WGA staining from the live parent form of Bb, since in their studies they did not detect N-linked glycans associated to outer surface proteins of Bb. Already in 1994, Hulinska *et al*. observed the specific binding of lectin to cystic forms (Brorson and Brorson, 1997). WGA dye reached the peptidoglycan of the live doxycycline treated control cells indicating the outer membrane damage caused by the antibiotic. However, WGA staining in RBs was observed only on the edges of RBs indicating a rearrangement on the cell wall components rather than membrane damage.

The background staining of WGA in Figure 2C could be explained by the GluNAc in BSK-II. GluNAc is needed in the culture medium, since Bb is not able to produce it by itself, even though GluNAc is an essential part of peptidoglycan cell wall and can be used as an energy source by the bacterium (Rhodes *et al.*, 2009). In fact, GluNAc is a primary constituent of chitin which makes up the tick cuticle and may thereby serve as an energy source for Bb while it is residing in the tick host (Fraser *et al.*, 1997).

On the other hand, collagen production was observed uniquely in biofilms (Figure 2C) indicating that this assembly of spirochetes truly is a pleomorphic form of Bb (Lembre *et al.*, 2012; Sapi *et al.*, 2012). Bb biofilms are special since they can develop in suspension even though biofilms commonly grow on surfaces. Collagen-like substances were observed to be essential to biofilm formation in *Legionella pneumophila* (Mallegol *et al*., 2012). *Legionella* collagen-like protein (Lcl) containing collagen-like motifs was examined to have a role in the adhesion of the biofilms as well as to most probably participate in cell-cell or cell-matrix interactions inside the biofilm. Perhaps collagen observed in Figure 2C might also have a role in the attachment of the biofilm components. Iodine solution stained glycogen granules in all forms of Bb, except for some reason in the doxycycline treated controls (Figure 2C). Perhaps the damage caused by the antibiotic caused the cells to lose their glycogen.

5.2 Coiling of the spirochete into a viable RB form

The step-wise model of the folding of spirochetes to RBs (Figure 3) is supported by previous findings of others (Brorson and Brorson, 1998; Murgia and Cinco, 2004; Al-Robaiy *et al*., 2010). For example, Murgia and Cinco (2004) illustarted a step-wise model of RB formation induced by H_2O_2. In the model, RB formation begins with a budding of the outer membrane, and folding of the protoplasmic cylinder follows. In addition, the protruding spirochetal tail in RBs was observed by Brorson and Brorson (1998).

Great flexibility of the outer membrane can be observed in Figure 3A when the outer membrane swells to accommodate the coiling protoplasmic cylinder inside. Flexibility of the outer membrane is needed for the folding process. Kudryashev *et al*. (2009) observed that at the sites where the protoplasmic cylinder forms protrusions, the peptidoglycan layer followed the curvature of the outer membrane instead of the protoplasmic cylinder. Further, they remarked the same phenomenon in the RBs, which they induced by anti-outer membrane protein A (OspA). In these RBs, the slime layer seemed to be intact and the peptidoglycan layer was observed adjacent to the outer membrane. This would allow the protoplasmic cylinder to coil quite freely during the RB formation. These observations are contradictive to the proposed molecular structure of Bb membranes by Cox *et al*. (1996) and Schröder *et al*. (2008), where the peptidoglycan layer is closely associated to the inner membrane of Bb.

The calculations on the surface to volume ratios of spirochetes and RBs (calculations 1-6 in Results) give insight to the changes observed in Figure 3. The difference in the diameter (2.8 ± 0.46 µm DIC vs ~2.4 µm TEM) might be explained by shrinking of the cells during sample processing for TEM thin sections. Spirochetes have much larger surface-area-to-volume ratio compared to RBs, 20 versus 2.1 (see calculations 3 and 6). This might be beneficial to the metabolically active spirochete form of Bb, since there is a large surface for scavenging nutrients from the environment, and the short distances inside the cell enable quick reactions. On the other hand, the metabolic activity of RBs is lower (Murgia and Cinco, 2004) and thereby they have no use for large surface-area-to-volume ratio. RBs do have a volume almost 20 times larger compared to spirochetes (see calculations 2 and 5) which indicates some changes in the permeability of the outer membrane that allows the

bacteria to swell. Probably, these changes are beneficial for short-term survival of harsh environmental conditions (Murgia and Cinco, 2004; Brorson *et al*., 2009).

5.3 Flagella are conserved in the RB form

Flagella is not lost during the RB formation (Figure 4) which supports the idea of RB as a pleomorphic structure from which the bacteria is able to revert back into the spirochetal shape (Brorson and Brorson, 1997; Murgian and Cinco, 2004; Brorson *et al*., 2009). The presence of flagella inside the cystic structures has also been previously observed by Brorson and Brorson (1997). TEM images (Figure 4B) suggested that the flagella are located next to the protoplasmic cylinder in RBs. Flagellar proteins act as antigens, so hiding them from the host's immune system in the periplasmic space is beneficial to the bacterium. In spirochetes, flagella participate in the movement, give general structure to Bb, and are essential to infectivity (Motaleb *et al*., 2000; Sultan *et al*., 2013) whereas in RBs, which are a metabolically inactive form (Murgia and Cinco, 2004), the participation in the movement of the bacterium is unlikely. In addition, the flagella are not essential to RB formation (Al-Robaiy *et al*., 2010).

Our results object to the findings of Brucket *et al.* (1995) who observed Bb RBs releasing flagella from the periplasmic space. The green fluorescence from the immunolabeled flagella in Figure 4 should be more dispersed if the flagella would be released. Instead, the flagella seem to follow the curvature of the protoplasmic cylinder (Figure 4). This model is supported by Kudrashev *et al.* (2009), who came to a conclusion that the peptidoglycan layer follows the curvature of the outer membrane.

5.4 Swollen protoplasmic cylinder a step in RB formation?

It would be intriguing to further examine the swelling phenomenon of the protoplasmic cylinders in human serum induced RBs. It seemed that human serum triggered the swelling since much less swelling of the protoplasmic cylinders was observed in the H_2O induced RBs (see Table 2), although this might be due the short incubation time, 2 h compared to 4 d. Also, human serum causes the form change from spirochetes into RBs while rabbit serum does not. Thereby, the complement is probably behind these events (van Dam *et al*., 1997). The incubation of RBs in both H_2O and human serum should be continued for a

longer period of time to observe if the swollen form would in fact present a final step in the RB formation process.

Brorson and Brorson (1998) observed that in RBs induced by incubation in distilled H_2O for one week, the spirochetal forms inside the RBs seemed to disappear and be replaced by a core structure. The RBs were able to revert back to mobile spirochetes even after 5 weeks incubation in H_2O, although the recovery took over 4 weeks in BSK-H medium (Brorson and Brorson, 1998). This would suggest that the swollen protoplasmic cylinders seen here (Figure 5) would also derive from the long incubation, 4 d in human serum compared to only 2 h in H_2O, and not be caused by the serum. The presence of RNA was confirmed in two weeks H_2O incubated RBs by acridine orange staining (Brorson and Brorson, 1998). The core structures inside RBs have been observed by others as well (Murgia and Cinco, 2004). The formation of core structures in H_2O induced Bb RBs was prevented when the cells were treated with metronidazole, a DNA attacking antibiotic (Brorson and Brorson, 1999). This could implicate that the swelling of the protoplasmic cylinder in RBs serves to enable Bb to stand unfavourable environmental conditions. At least it seems to indicate that these forms are viable and keep their ability to revert back to spirochetes, even with the swollen protoplasmic cylinders.

5.5 Stressful conditions increased vesicle formation

The vesicle forms demonstrated in Figure 6 have also been observed by others, but the role of the vesicles is still controversial. For example, 3 h H_2O RBs studied by Brorson and Brorson (1998) were observed to secrete pearl-like vesicles (Figure 6E). Similarly, vesicle formation was observed in RBs incubated for two weeks in H_2O (Brorson and Brorson, 1998. Also Vancová *et al*. (2005) reported Bb vesicles in pearl and rod shapes with a diameter ranging between 50 to 200 nm. In addition, they observed a tendency of self-aggregation of the vesicles (compare to Figure 6G and H).

Vesicle formation is likely to be increased by unfavourable environmental conditions (Alban *et al*., 2000). Here the environment was created by 4 d incubation in human serum and an increase in vesicle formation was not observed so markedly in 2 h H_2O RBs. In the future, it would be interesting to see if the vesicles have an immunological role in Lyme disease. An interesting possibility was examined by Crowley *et al.* in 2013 who claimed

that vesicles are used for two-way lipid exchange between Bb and the mammalian host. Bb is unable to produce cholesterol, but can acquire it from the mammalian host, and *vice versa* free cholesterol or cholesterol-glycolipids from Bb may be transferred to host cells. The interaction of Bb outer membrane vesicles and mammalian cells was also demonstrated by Shoberg and Thomas (1993). This could provide an explanation for the chronic state of Lyme disease, since Bb antigens could be transferred to the cells of the patient causing the immune system react to body's own cells. Another possible role for the vesicles could be in reproduction (Briers *et al.,* 2012). Briers *et al.* (2012) demonstrated how intracellular vesicles were used as a reproductive element in cell wall deficient L-form bacteria. L-form bacteria share a similar spherical structure with the Bb RBs, but have a damaged cell wall.

5.6 Increased protein expression in RBs

The genome data of Bb B31 suggests that the bacterium has proteins of molecular weight from 3.365 kDa to 254.242 kDa (Fraser *et al*., 1997) as seen also in Figure 7. In the 2D PAGE studies of Alban *et al.* (2000) and Al-Robaiy *et al.* (2010), comparing spirochete versus RPMI serum starved and H_2O induced RBs respectively, no protein spots were detected above 66 kDa. On the other hand, the 15 proteins (spots 11–16 and 18–26 in Table 3) that had elevated expression in RBs were of molecular weight 15–40 kDa. Three proteins with elevated protein expression in RB form (spots 11, 18 and 19, see Table 3) corresponded to the 2D PAGE results of Alban *et al*. (2000). Al-Robaiy *et al*. (2010) studied extensively 6–16 kDa proteins of Bb spirochetes and RBs with mass spectrometry, and did not find any differences between the forms. In contrast to their results, two 15 kDa proteins (spots 25 and 26 in Figure 7 and Table 3) with increased expression in RBs, were detected. However, few protein spots were even detected on the molecular weight area 6–16 kDa in the 2D PAGE gels (Figure 7).

Two hours incubation that was utilized in 2D experiments here might not be a sufficiently long time for studying changes in the protein expression. However, the change from spirochete to RBs takes place in minutes (Brorson and Brorson, 1998). No decrease in protein expression of the RB form was observed (Figure 7), which might have been expected if RB would be a cell wall deficient form of Bb. Instead, an up-regulation of 15 proteins was seen in the RB form (Table 3). The roles of these proteins should be further

studied. These proteins might be related to metabolic inactivity, shape formation or perhaps provide ways to hide from the immune defense or antibiotic treatment as suggested by others (Murgia *et al*., 2002; Miklossy *et al*., 2008; Brorson *et al*. 2009). For clinical relevance, it would be interesting to study the RBs induced by human serum in various time points with 2D PAGE method. Environmental conditions have a large impact on the protein expression of Bb since the bacterium is accustomed to live in different hosts and is able to adjust its protein expression according to environmental factors (Alban *et al*., 2000).

5.7 Individual antibody-antigen responses of spirochete and RBs

Alban *et al*. (2000) observed reduced antigenicity of flagellum protein (41 kDa) and a protein with molecular weight of 46 kDa in 48 h serum starved RBs. However, as shown in Figure 4, the flagella are still present in the RB forms and the antibody response at 41 kDa was repeatedly higher in RBs in the western blots (see Table 4). In the experiments here, Lyme patient sera seemed to be more reactive towards RBs than to spirochetes suggesting that these patients have encountered RBs, which indicates that RBs are clinically relevant (Table 4).

Al-Robaiy *et al.* (2010) studied the antigenicity of RBs induced in H_2O for 1-32 days and observed reduced protein-antibody reactivity with the advanced age of the RBs. In this study, the RBs were incubated only 2h in H_2O. In addition, compared to samples separated by 2D PAGE (Figure 7), fewer protein spots from spirochete and RB samples were available for comparison (Figure 8). Nevertheless, differences in the intensity of the response to patient serum between spirochetes and RBs were repeatedly observed (Table 4). In the end, the antibody-antigen response depends on the serum antibodies that may vary greatly between sera (Dressler *et al.*, 1993) as seen also in Table 4 in the intensity differences of the bands. Differences in the antibody-antigen reactions between sera are not surprising considering the huge variability of lipoprotein expression that Bb possesses (Cluss and Boothby, 1990; Montgomery *et al*., 1996). Out of 150 lipoproteins only some are expressed at a certain time and Bb can change their expression, hence naturally the antibodies are also produced against different antigens (Shcnarr *et al*., 2006).

Many patient sera seemed to have a stronger response to RBs than to spirochetes (Figure 8 and Table 4). This might be due to the rearrangement of the outer membrane in the process of RB formation since, for example, peptidoglycan was observed to become accessible on the surface of the RBs with WGA staining (Figure 2C). In addition, it would be interesting to further study whether the increased vesicle formation induced by incubation in human serum could have an immunological purpose (Figure 6). Possibly the vesicles make some antigens exposed simply by transferring them from inside the cells to the outside or perhaps some proteins get re-processed in the vesicles providing new epitopes of the antigens (Deatherage and Cookson, 2012).

Western blots are commonly used for diagnosis of Lyme disease. Five of the ten protein bands should be present in the IgG blot: 18, 21, 28, 30, 39, 41, 45, 58, 66 and 93 kDa (Dressler *et al*., 1993) for diagnosis of Lyme disease, and similar bands were seen in western blots here for both spirochetes and RBs (Table 4). Special interest has been stressed on the bands 18, 21 and 93 kDa by Dressler *et al*. (1993) since no cross-reactivity with other diseases was observed. These bands were also present here in at least six blots out of seven (see Table 4). Volkman *et al*. (1991) suggested that the 93 kDa protein would be anchored within the protoplasmic cylinder and perhaps have a role in the anchorage of the flagella. RBs had a response to the 93 kDa protein antibody from the sera indicating that the anchorage proteins of the flagella would be conserved in this form. The western blots seem to include bands for OspA (31 kDa), OspB (34 kDa) and flagellin (41 kDa), which are mentioned by Bruck *et al*. (1995) as common antigens in Lyme disease. However, care must be taken when interpreting the results of western blots since the estimation of molecular weight is subjective, as is the decision on the interpretation of faint bands (Dressler *et al*., 1993). Further problems arise from the insensitivity, since several proteins might migrate on the same band according to their molecular weights as seen here when comparing the 2D PAGE gels to western blot membranes (Figures 7 and 8).

5.8 Round bodies are not cell wall deficient nor cyst forms

Numerous articles exist where cell wall deficient forms of Bb have been studied (Bruck *et al*., 1995; Mursic *et al*., 1999; Brorson *et al*., 2009; Stricker and Johnson, 2011). These studies claim that the outer cell wall of Bb is compromised although it is not

experimentally shown (Brorson *et al*., 2009). Changes in the cell envelope of Bb RB forms were seen in this Master's thesis also, since the peptidoglycan layer became exposed on the RB surface (Figure 2C, WGA staining). Furthermore, differences in the protein profiles between spirochetes and RBs were observed (Figure 7). However, no diminution of the protein expression in RB form was detected (Table 3), which might be expected if the outer membrane would be damaged. Also Bruck *et al*. (1995) did not observe a change in the outer surface proteins, OspA and OspB, expression between spirochetes and spheroplasts (RBs). The spheroplast term was based on the release of flagella from the periplasmic space and increased vesicle formation, although undamaged double membranes were perceived in the TEM thin sections. Most probably, the release of flagella was due to the sample preparation for PTA staining. The same phenomenon was observed here when samples were not fixed prior to PTA staining. Flagella were not seen if fixing was carried out (data not shown, but see Figure 1 for fixed PTA stained Bb forms). Increased vesicle formation in stressful conditions, caused by human serum, was observed but despite that the double membranes seemed to be undamaged (Figure 6). One of the reasons why terms such as spheroplast or L-form have been utilized to refer to Bb RBs is the inability of these forms to replicate. However, there is no reason why the cell wall should be compromised for this. RB might as well just be a metabolically inactive pleomorphic form that allows Bb to survive environmentally compromised conditions (Murgia and Cinco, 2004; Brorson *et al*., 2009).

One problem with the studies on the alternative forms of Bb is the various methods to induce them. For example, the spheroplast or L-phase forms have been induced by inadequate culture media, pH alterations, lysozyme treatment, antibodies, complement, as well as with antibiotics (Mursic *et al*., 1996). Thereby, it is not surprising that controversy exists about these forms. Surely, by antibiotic treatment the cell wall may become compromised, as seen also in this study where doxycycline treated cells were used as a control (Figure 2 and Figure 8). Mursic *et al*. (1996) suggested in accordance to Bruck *et al*. (1995) that the spheroplast forms with damaged outer cell wall and released flagella could describe the bacterial cells under the attack of host immune system. However, no outer membrane damage was observed in the TEM images even with 4d incubation in human serum, although increased vesicle formation or swelling of the protoplasmic cylinders was observed (Figure 5 and 6).

Cysts would be a suitable term to describe Bb in the spherical form in a sense that cysts are typically considered as dormant and metabolically inactive forms of bacteria, which it can use to survive unfavourable environmental conditions (Miklossy *et al*., 2008). However, thickening of cell walls is often associated into bacterial cyst formation, which was not observed in TEM micrographs (Figure 3). The double membrane structure is conserved and intact in the RB forms (see Figure 3B), which explains why the spheroplast term is inappropriate for describing RBs. The view of RBs as a viable, pleomorphic form of Bb is shared by other researches on the field, see for example Margulis *et al*. (2009), Brorson and Brorson (1997), and Brorson *et al.* (2009).

Conclusion

The pleomorphic forms of Bb have unique characteristics. Biofilms can be detected by collagen binding dyes whereas RBs can be spotted with lectins, since peptidoglycan becomes exposed at the RB surface. These observations could be used in more specific detection of Bb *in vitro* and perhaps in diagnosis of Lyme disease in the future. Human serum induces RB formation and seems to cause increased vesicle formation and swelling of the protoplasmic cylinder. The role of RBs and the released vesicles in the pathology of Lyme disease should be further examined. Lipid membranes are undamaged and the flagella stay intact in RBs indicating that RBs are a clinically significant form of Bb. The protein expression changes when spirochetes obtain RB form. The proteins whose expression is higher in RBs might be responsible for the adjustment to the unfavourable environmental conditions. RBs are able to induce an immunological response in Lyme disease patients and should be taken into account in the diagnosis of the patients.

References

Aberer, E., and P.H. Duray. 1991. Morphology of Borrelia burgdorferi: structural patterns of cultured borreliae in relation to staining methods. J.Clin.Microbiol. 29:764-772.

Adelson, M.E., R.V. Rao, R.C. Tilton, K. Cabets, E. Eskow, L. Fein, J.L. Occi, and E. Mordechai. 2004. Prevalence of Borrelia burgdorferi, Bartonella spp., Babesia microti, and Anaplasma phagocytophila in Ixodes scapularis ticks collected in Northern New Jersey. J.Clin.Microbiol. 42:2799-2801.

Alban, P.S., P.W. Johnson, and D.R. Nelson. 2000. Serum-starvation-induced changes in protein synthesis and morphology of Borrelia burgdorferi. *Microbiology.* 146 (Pt 1):119-127.

Al-Robaiy, S., H. Dihazi, J. Kacza, J. Seeger, J. Schiller, D. Huster, J. Knauer, and R.K. Straubinger. 2010. Metamorphosis of Borrelia burgdorferi organisms--RNA, lipid and protein composition in context with the spirochetes' shape. J.Basic Microbiol. 50 Suppl 1:S5-17.

Banerjee, A., P. Majumder, S. Sanyal, J. Singh, K. Jana, C. Das, and D. Dasgupta. 2014. The DNA intercalators ethidium bromide and propidium iodide also bind to core histones. FEBS Open Bio. 4:251-259.

Barbour, A.G. 1984. Isolation and cultivation of Lyme disease spirochetes. *Yale J.Biol.Med.* 57:521-525.

Barbour, A.G., and S.F. Hayes. 1986. Biology of Borrelia species. *Microbiol.Rev.* 50:381-400.

Briers, Y., T. Staubli, M.C. Schmid, M. Wagner, M. Schuppler, and M.J. Loessner. 2012. Intracellular vesicles as reproduction elements in cell wall-deficient L-form bacteria. PLoS One. 7:e38514.

Brorson, O., and S.H. Brorson. 1999. An *in vitro* study of the susceptibility of mobile and cystic forms of Borrelia burgdorferi to metronidazole. *Apmis.* 107:566-576.

Brorson, O., and S.H. Brorson. 1998. A rapid method for generating cystic forms of Borrelia burgdorferi, and their reversal to mobile spirochetes. *Apmis.* 106:1131-1141.

Brorson, O., and S.H. Brorson. 1997. Transformation of cystic forms of Borrelia burgdorferi to normal, mobile spirochetes. *Infection.* 25:240-246.

Brorson, O., S.H. Brorson, J. Scythes, J. MacAllister, A. Wier, and L. Margulis. 2009. Destruction of spirochete Borrelia burgdorferi round-body propagules (RBs) by the antibiotic tigecycline. *Proc.Natl.Acad.Sci.U.S.A.* 106:18656-18661.

Bruck, D.K., M.L. Talbot, R.G. Cluss, and J.T. Boothby. 1995. Ultrastructural characterization of the stages of spheroplast preparation of Borrelia burgdorferi. *J.Microbiol.Methods.* 23:219-228.

Burgdorfer, W., A.G. Barbour, S.F. Hayes, J.L. Benach, E. Grunwaldt, and J.P. Davis. 1982. Lyme disease-a tick-borne spirochetosis? *Science.* 216:1317-1319.

Busch, U., C. Hizo-Teufel, R. Boehmer, V. Fingerle, H. Nitschko, B. Wilske, and V. Preac-Mursic. 1996. Three species of Borrelia burgdorferi sensu lato (B. burgdorferi sensu stricto, B afzelii, and B. garinii) identified from cerebrospinal fluid isolates by pulsed-field gel electrophoresis and PCR. *J.Clin.Microbiol.* 34:1072-1078.

CDC, USA. Lyme disease cases per year. http://www.cdc.gov/lyme/stats/chartstables/casesbyyear.html. 28.09.2014.

Cluss, R.G., and J.T. Boothby. 1990. Thermoregulation of protein synthesis in Borrelia burgdorferi. Infect.Immun. 58:1038-1042.

Cox, D.L., D.R. Akins, K.W. Bourell, P. Lahdenne, M.V. Norgard, and J.D. Radolf. 1996. Limited surface exposure of Borrelia burgdorferi outer surface lipoproteins. *Proc.Natl.Acad.Sci.U.S.A.* 93:7973-7978.

Crowley, J.T., A.M. Toledo, T.J. LaRocca, J.L. Coleman, E. London, and J.L. Benach. 2013. Lipid exchange between Borrelia burgdorferi and host cells. *PLoS Pathog.* 9:e1003109.

Deatherage, B.L., and B.T. Cookson. 2012. Membrane vesicle release in bacteria, eukaryotes, and archaea: a conserved yet underappreciated aspect of microbial life. Infect.Immun. 80:1948-1957.

de Silva, A.M., S.R. Telford 3rd, L.R. Brunet, S.W. Barthold, and E. Fikrig. 1996. Borrelia burgdorferi OspA is an arthropod-specific transmission-blocking Lyme disease vaccine. *J.Exp.Med.* 183:271-275.

Dressler, F., J.A. Whalen, B.N. Reinhardt, and A.C. Steere. 1993. Western blotting in the serodiagnosis of Lyme disease. *J.Infect.Dis.* 167:392-400.

Elias, A.F., P.E. Stewart, D. Grimm, M.J. Caimano, C.H. Eggers, K. Tilly, J.L. Bono, D.R. Akins, J.D. Radolf, T.G. Schwan, and P. Rosa. 2002. Clonal polymorphism of Borrelia burgdorferi strain B31 MI: implications for mutagenesis in an infectious strain background. *Infect.Immun.* 70:2139-2150.

Feder, H.M.,Jr, M. Abeles, M. Bernstein, D. Whitaker-Worth, and J.M. Grant-Kels. 2006. Diagnosis, treatment, and prognosis of erythema migrans and Lyme arthritis. *Clin.Dermatol.* 24:509-520.

Ferdows, M.S., and A.G. Barbour. 1989. Megabase-sized linear DNA in the bacterium Borrelia burgdorferi, the Lyme disease agent. Proc.Natl.Acad.Sci.U.S.A. 86:5969-5973.

Fraser, C.M., S. Casjens, W.M. Huang, G.G. Sutton, R. Clayton, R. Lathigra, O. White, K.A. Ketchum, R. Dodson, E.K. Hickey, M. Gwinn, B. Dougherty, J.F. Tomb, R.D. Fleischmann, D. Richardson, J. Peterson, A.R. Kerlavage, J. Quackenbush, S. Salzberg, M. Hanson, R. van Vugt, N. Palmer, M.D. Adams, J. Gocayne, J. Weidman, T. Utterback, L. Watthey, L. McDonald, P. Artiach, C. Bowman, S. Garland, C. Fuji, M.D. Cotton, K. Horst, K. Roberts, B. Hatch, H.O. Smith, and J.C. Venter. 1997. Genomic sequence of a Lyme disease spirochaete, Borrelia burgdorferi. *Nature.* 390:580-586.

Garland, F., D.E. Graves, L.W. Yielding, and H.C. Cheung. 1980. Comparative studies of the binding of ethidium bromide and its photoreactive analogues to nucleic acids by fluorescence and rapid kinetics. Biochemistry. 19:3221-3226.

Girschick, H.J., H. Morbach, and D. Tappe. 2009. Treatment of Lyme borreliosis. *Arthritis Res.Ther.* 11:258.

Goldstein, S.F., K.F. Buttle, and N.W. Charon. 1996. Structural analysis of the Leptospiraceae and Borrelia burgdorferi by high-voltage electron microscopy. J.Bacteriol. 178:6539-6545.

Greenspan, P., E.P. Mayer, and S.D. Fowler. 1985. Nile red: a selective fluorescent stain for intracellular lipid droplets. *J.Cell Biol.* 100:965-973.

Grimm, D., K. Tilly, R. Byram, P.E. Stewart, J.G. Krum, D.M. Bueschel, T.G. Schwan, P.F. Policastro, A.F. Elias, and P.A. Rosa. 2004. Outer-surface protein C of the Lyme disease spirochete: a protein induced in ticks for infection of mammals. *Proc.Natl.Acad.Sci.U.S.A.* 101:3142-3147.

Hovind-Hougen, K. 1984. Ultrastructure of spirochetes isolated from Ixodes ricinus and Ixodes dammini. *Yale J.Biol.Med.* 57:543-548.

Hubalek, Z., J. Halouzka, and M. Heroldova. 1998. Growth temperature ranges of Borrelia burgdorferi sensu lato strains. J.Med.Microbiol. 47:929-932.

Iyer, R., P. Mukherjee, K. Wang, J. Simons, G.P. Wormser, and I. Schwartz. 2013. Detection of Borrelia burgdorferi nucleic acids after antibiotic treatment does not confirm viability. *J.Clin.Microbiol.* 51:857-862.

Jaulhac, B., R. Heller, F.X. Limbach, Y. Hansmann, D. Lipsker, H. Monteil, J. Sibilia, and Y. Piemont. 2000. Direct molecular typing of Borrelia burgdorferi sensu lato species in synovial samples from patients with lyme arthritis. *J.Clin.Microbiol.* 38:1895-1900.

Johnson, R.C., F.W. Hyde, and C.M. Rumpel. 1984. Taxonomy of the Lyme disease spirochetes. Yale J.Biol.Med. 57:529-537.

Kersten, A., C. Poitschek, S. Rauch, and E. Aberer. 1995. Effects of penicillin, ceftriaxone, and doxycycline on morphology of Borrelia burgdorferi. *Antimicrob.Agents Chemother.* 39:1127-1133.

Kraiczy, P., C. Skerka, V. Brade, and P.F. Zipfel. 2001. Further characterization of complement regulator-acquiring surface proteins of Borrelia burgdorferi. Infect.Immun. 69:7800-7809.

Kudryashev, M., M. Cyrklaff, W. Baumeister, M.M. Simon, R. Wallich, and F. Frischknecht. 2009. Comparative cryo-electron tomography of pathogenic Lyme disease spirochetes. *Mol.Microbiol.* 71:1415-1434.

Lembre, P., C. Lorentz and P. Di Martino. 2012. Exopolysaccharides of the Biofilm Matrix: A Complex Biophysical World, The Complex World of Polysaccharides. Dr. D. N. Karunaratne, editor. InTech. 371-392.

Lemkin P.F., G. Thornwall, J. Evans. 2005. Comparing 2-D Electrophoretic Gels Across Internet Databases. J. Walker, editor. The Protein Protocols Handbook. Humana Press Inc. Totowa. NJ. 279-305.

Liang, F.T., E.L. Brown, T. Wang, R.V. Iozzo, and E. Fikrig. 2004. Protective niche for Borrelia burgdorferi to evade humoral immunity. *Am.J.Pathol.* 165:977-985.

Liang, F.T., M.B. Jacobs, L.C. Bowers, and M.T. Philipp. 2002. An immune evasion mechanism for spirochetal persistence in Lyme borreliosis. *J.Exp.Med.* 195:415-422.

Mallegol, J., C. Duncan, A. Prashar, J. So, D.E. Low, M. Terebeznik, and C. Guyard. 2012. Essential roles and regulation of the Legionella pneumophila collagen-like adhesin during biofilm formation. PLoS One. 7:e46462.

Margulis, L., A. Maniotis, J. MacAllister, J. Scythes, O. Brorson, J. Hall, W. Krumbein, and M. Chapman. 2009. Spirochete round bodies Syphilis, Lyme disease & AIDS: Resurgence of "the great imitator" • ? *Symbiosis.* 47:51-58.

Meriläinen, L., A. Herranen, and L. Gilbert. 2014. Morphological and biochemical features of Borrelia burgdorferi pleomorphic forms. Manuscript.

Michelet, L., S. Delannoy, E. Devillers, G. Umhang, A. Aspan, M. Juremalm, J. Chirico, F.J. van der Wal, H. Sprong, T.P. Boye Pihl, K. Klitgaard, R. Bodker, P. Fach, and S. Moutailler. 2014. High-throughput screening of tick-borne pathogens in Europe. Front.Cell.Infect.Microbiol. 4:103.

Miklossy, J., S. Kasas, A.D. Zurn, S. McCall, S. Yu, and P.L. McGeer. 2008. Persisting atypical and cystic forms of Borrelia burgdorferi and local inflammation in Lyme neuroborreliosis. *J.Neuroinflammation.* 5:40-2094-5-40.

Montgomery, R.R., S.E. Malawista, K.J. Feen, and L.K. Bockenstedt. 1996. Direct demonstration of antigenic substitution of Borrelia burgdorferi ex vivo: exploration of the paradox of the early immune response to outer surface proteins A and C in Lyme disease. *J.Exp.Med.* 183:261-269.

Motaleb, M.A., L. Corum, J.L. Bono, A.F. Elias, P. Rosa, D.S. Samuels, and N.W. Charon. 2000. Borrelia burgdorferi periplasmic flagella have both skeletal and motility functions. *Proc.Natl.Acad.Sci.U.S.A.* 97:10899-10904.

Murgia, R., and M. Cinco. 2004. Induction of cystic forms by different stress conditions in Borrelia burgdorferi. *Apmis.* 112:57-62.

Murgia, R., C. Piazzetta, and M. Cinco. 2002. Cystic forms of Borrelia burgdorferi sensu lato: induction, development, and the role of RpoS. *Wien.Klin.Wochenschr.* 114:574-579.

Mursic, V.P., G. Wanner, S. Reinhardt, B. Wilske, U. Busch, and W. Marget. 1996. Formation and cultivation of Borrelia burgdorferi spheroplast-L-form variants. *Infection.* 24:218-226.

National Institute of Health and Welfare, Finland. http://www.thl.fi/ttr/gen/rpt/tilastot.html. 28.09.2014.

Nau, R., H.J. Christen, and H. Eiffert. 2009. Lyme disease--current state of knowledge. Dtsch.Arztebl Int. 106:72-81; quiz 82, I.

Pal, U., X. Yang, M. Chen, L.K. Bockenstedt, J.F. Anderson, R.A. Flavell, M.V. Norgard, and E. Fikrig. 2004. OspC facilitates Borrelia burgdorferi invasion of Ixodes scapularis salivary glands. *J.Clin.Invest.* 113:220-230.

Picken, R.N., F. Strle, M.M. Picken, E. Ruzic-Sabljic, V. Maraspin, S. Lotric-Furlan, and J. Cimperman. 1998. Identification of three species of Borrelia burgdorferi sensu lato (B. burgdorferi sensu stricto, B. garinii, and B. afzelii) among isolates from acrodermatitis chronica atrophicans lesions. *J.Invest.Dermatol.* 110:211-214.

Rasband, W.S., ImageJ, U. S. National Institutes of Health, Bethesda, Maryland, USA, http://imagej.nih.gov/ij/, 1997-2014.

Rhodes, R.G., W. Coy, and D.R. Nelson. 2009. Chitobiose utilization in Borrelia burgdorferi is dually regulated by RpoD and RpoS. *BMC Microbiol.* 9:108-2180-9-108.

Rosa, P.A., K. Tilly, and P.E. Stewart. 2005. The burgeoning molecular genetics of the Lyme disease spirochaete. *Nat.Rev.Microbiol.* 3:129-143.

Sachsenmeier, K.F., K. Schell, L.W. Morrissey, D.R. Pennell, R.M. West, S.M. Callister, and R.F. Schell. 1992. Detection of borreliacidal antibodies in hamsters by using flow cytometry. J.Clin.Microbiol. 30:1457-1461.

Sapi, E., S.L. Bastian, C.M. Mpoy, S. Scott, A. Rattelle, N. Pabbati, A. Poruri, D. Burugu, P.A. Theophilus, T.V. Pham, A. Datar, N.K. Dhaliwal, A. MacDonald, M.J. Rossi, S.K. Sinha, and D.F. Luecke. 2012. Characterization of biofilm formation by Borrelia burgdorferi *in vitro*. *PLoS One.* 7:e48277.

Sapi, E., N. Kaur, S. Anyanwu, D.F. Luecke, A. Datar, S. Patel, M. Rossi, and R.B. Stricker. 2011. Evaluation of in-vitro antibiotic susceptibility of different morphological forms of Borrelia burgdorferi. *Infect.Drug Resist.* 4:97-113.

Schnarr, S., J.K. Franz, A. Krause, and H. Zeidler. 2006. Infection and musculoskeletal conditions: Lyme borreliosis. *Best Pract.Res.Clin.Rheumatol.* 20:1099-1118.

Schröder, N.W., U. Schombel, H. Heine, U.B. Gobel, U. Zahringer, and R.R. Schumann. 2003. Acylated cholesteryl galactoside as a novel immunogenic motif in Borrelia burgdorferi sensu stricto. J.Biol.Chem. 278:33645-33653.

Schröder, N.W., J. Eckert, G. Stubs, and R.R. Schumann. 2008. Immune responses induced by spirochetal outer membrane lipoproteins and glycolipids. *Immunobiology.* 213:329-340.

Schwan, T.G., J. Piesman, W.T. Golde, M.C. Dolan, and P.A. Rosa. 1995. Induction of an outer surface protein on Borrelia burgdorferi during tick feeding. *Proc.Natl.Acad.Sci.U.S.A.* 92:2909-2913.

Shoberg, R.J., and D.D. Thomas. 1993. Specific adherence of Borrelia burgdorferi extracellular vesicles to human endothelial cells in culture. *Infect.Immun.* 61:3892-3900.

Stanek, G., G.P. Wormser, J. Gray, and F. Strle. 2012. Lyme borreliosis. Lancet. 379:461-473.

Sterba, J., M. Vancova, N. Rudenko, M. Golovchenko, T.L. Tremblay, J.F. Kelly, C.R. MacKenzie, S.M. Logan, and L. Grubhoffer. 2008. Flagellin and outer surface proteins from Borrelia burgdorferi are not glycosylated. *J.Bacteriol.* 190:2619-2623.

Stricker, R.B., and L. Johnson. 2011. Lyme disease: the next decade. *Infect.Drug Resist.* 4:1-9.

Sultan, S.Z., A. Manne, P.E. Stewart, A. Bestor, P.A. Rosa, N.W. Charon, and M.A. Motaleb. 2013. Motility is crucial for the infectious life cycle of Borrelia burgdorferi. *Infect.Immun.* 81:2012-2021.

Suzuki, T., K. Fujikura, T. Higashiyama, and K. Takata. 1997. DNA staining for fluorescence and laser confocal microscopy. J.Histochem.Cytochem. 45:49-53.

Takayama, K., R.J. Rothenberg, and A.G. Barbour. 1987. Absence of lipopolysaccharide in the Lyme disease spirochete, Borrelia burgdorferi. *Infect.Immun.* 55:2311-2313.

Thammasri K., A. Campillo, L. Meriläinen, A. Schwarzbach, P. Garcia-Nogales, and L. Gilbert. 2014. Advance ELISA with multiplex antigen array for the diagnosis of Tick-borne disease. Manuscript.

Vancova, M., J. Nebesarova, and L. Grubhoffer. 2005. Lectin-binding characteristics of a Lyme borreliosis spirochete Borrelia burgdorferi sensu stricto. *Folia Microbiol.(Praha).* 50:229-238.

van Dam, A.P., A. Oei, R. Jaspars, C. Fijen, B. Wilske, L. Spanjaard, and J. Dankert. 1997. Complement-mediated serum sensitivity among spirochetes that cause Lyme disease. Infect.Immun. 65:1228-1236.

Volkman, D.J., B.J. Luft, P.D. Gorevic, J. Schultz, and L. Padovano. 1991. Characterization of an immunoreactive 93-kDa core protein of Borrelia burgdorferi with a human IgG monoclonal antibody. J.Immunol. 146:3177-3182.